

2016

Planetary Nebula Associations with Star Clusters in the Andromeda Galaxy

Yasmine Kahvaz
kahvaz@marshall.edu

Follow this and additional works at: <http://mds.marshall.edu/etd>



Part of the [Stars, Interstellar Medium and the Galaxy Commons](#)

Recommended Citation

Kahvaz, Yasmine, "Planetary Nebula Associations with Star Clusters in the Andromeda Galaxy" (2016). *Theses, Dissertations and Capstones*. 1052.
<http://mds.marshall.edu/etd/1052>

This Thesis is brought to you for free and open access by Marshall Digital Scholar. It has been accepted for inclusion in Theses, Dissertations and Capstones by an authorized administrator of Marshall Digital Scholar. For more information, please contact zhangj@marshall.edu, martj@marshall.edu.

**PLANETARY NEBULA ASSOCIATIONS WITH STAR CLUSTERS IN THE
ANDROMEDA GALAXY**

A thesis submitted to
the Graduate College of
Marshall University
In partial fulfillment of
the requirements for the degree of
Master of Physical and Applied Science
in
Physics
by

Yasmine Kahvaz

Approved by

Dr. Timothy Hamilton, Committee Chairperson

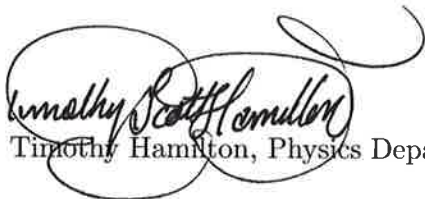
Dr. Maria Babiuc Hamilton

Dr. Ralph Oberly

Marshall University
Dec 2016


APPROVAL OF THESIS/DISSERTATION

We, the faculty supervising the work of Yasmine Kahvaz, affirm that the thesis, Planetary Nebula Associations With Star Clusters in the Andromeda Galaxy, meets the high academic standards for original scholarship and creative work established by the Physics Department and the College of Science. This work also conforms to the editorial standards of our discipline and the Graduate College of Marshall University. With our signatures, we approve the manuscript for publication.


Dr. Timothy Hamilton, Physics Department


Committee Chairperson

Dec. 7 2016
Date


Dr. Maria Babiuc Hamilton, Physics Department

Committee Member

Date


Dr. Ralph Oberly, Physics Department

Committee Member

Date

12-7-16

ACKNOWLEDGEMENTS

I would like to thank my advisor, Dr. Timothy Hamilton at Shawnee State University, for his guidance, advice and support for all the aspects of this project. My committee, including Dr. Timothy Hamilton, Dr. Maria Babiuc Hamilton, and Dr. Ralph Oberly, provided a review of this thesis. This research has made use of the following databases: The Local Group Survey (lowell.edu/users/massey/lgsurvey.html) and the PHAT Survey (archive.stsci.edu/prepds/phat/). I would also like to thank the entire faculty of the Physics Department of Marshall University for being there for me every step of the way through my undergrad and graduate degree years.

CONTENTS

List of Figures	vi
List of Tables	vii
Abstract	ix
Chapter 1 THE INTRODUCTION	1
1.1 Background	1
1.2 Analyzing Stars With the Hertzsprung-Russell Diagram	2
1.3 Overview of Stellar Evolution	3
1.4 Planetary Nebula Formation	5
1.5 Associations Between Planetary Nebulae and Star Clusters	6
1.6 Previous Searches for Planetary Nebula—Cluster Associations	6
Chapter 2 DATA SETS	10
2.1 Local Group Survey	10
2.2 Panchromatic Hubble Andromeda Treasury	10
Chapter 3 Methods	14
3.1 Object Identification	14
3.1.1 Distinguishing PNe From Stars	14
3.1.2 Finding Stellar Clusters	16
3.2 Photometry	17
3.2.1 F475W-[OIII] magnitude relation	20
3.2.2 Chance Alignments	21
Chapter 4 RESULTS	23
4.1 Planetary Nebula Luminosity Function	23
4.2 PN 609	23
4.3 PN 457	26

Chapter 5	DISCUSSION AND CONCLUSION	33
5.1	Discussion	33
5.1.1	PN 609	34
5.1.2	PN 457	34
5.2	Future Work	36
5.3	Conclusions	36
Appendix A	LIST OF PN CANDIDATES FOUND IN M31	38
Appendix B	TABLE OF PN PARAMETERS	59
Appendix C	Letter from Institutional Research Board	73
References	74
Vita	76

LIST OF FIGURES

1.1 Hertzprung-Russell diagram of a star cluster	3
1.2 H-R diagram of PN progenitor star evolution	9
2.1 Overall area of M31 covered by the Local Group Survey	11
2.2 Linear relationship between m_{5007} and F475W magnitudes	13
3.1 Area of M31 covered by the Local Group Survey images	15
3.2 PN candidate distribution in M31	17
3.3 PHAT survey layout of the 23 image bricks on M31	18
4.1 The luminosity function of the PNe candidate catalog	24
4.2 The luminosity function of PNe module	24
4.3 The logarithmic luminosity function of PNe candidate catalog	25
4.4 The logarithmic luminosity function of PNe module	25
4.5 PHAT view broad-band of PN609 and its cluster	26
4.6 LGS emission-line view of PN 609	27
4.7 Color-mag diagram of region around PN 609	28
4.8 PN 609 and cluster	29
4.9 PN 609 and cluster in F475W filter of PHAT image	29
4.10 PN 457 in LGS images	30
4.11 PN 457 and clusters in PHAT images	31
4.12 Color-mag diagram for PN 457	32
5.1 Distribution of open clusters in only 6 fields of M31	35

LIST OF TABLES

3.1 Local Group Survey Images Used in Making of Color Images	16
3.2 PHAT Survey Images Used to Find PN/OC Association Candidates	22
4.1 PN/OC Association Candidates	23
4.2 PN609 Parameters	26
4.3 PN457 Parameters	27
A.1 PN Candidate Coordinates	39
A.1 PN Candidate Coordinates	40
A.1 PN Candidate Coordinates	41
A.1 PN Candidate Coordinates	42
A.1 PN Candidate Coordinates	43
A.1 PN Candidate Coordinates	44
A.1 PN Candidate Coordinates	45
A.1 PN Candidate Coordinates	46
A.1 PN Candidate Coordinates	47
A.1 PN Candidate Coordinates	48
A.2 PN Candidate Descriptions	49
A.2 PN Candidate Descriptions	50
A.2 PN Candidate Descriptions	51
A.2 PN Candidate Descriptions	52
A.2 PN Candidate Descriptions	53
A.2 PN Candidate Descriptions	54
A.2 PN Candidate Descriptions	55
A.2 PN Candidate Descriptions	56
A.2 PN Candidate Descriptions	57
A.2 PN Candidate Descriptions	58

B.1 PN Candidate Photometry	60
B.1 PN Candidate Photometry	61
B.1 PN Candidate Photometry	62
B.1 PN Candidate Photometry	63
B.1 PN Candidate Photometry	64
B.1 PN Candidate Photometry	65
B.1 PN Candidate Photometry	66
B.1 PN Candidate Photometry	67
B.1 PN Candidate Photometry	68
B.1 PN Candidate Photometry	69
B.1 PN Candidate Photometry	70
B.1 PN Candidate Photometry	71
B.1 PN Candidate Photometry	72

ABSTRACT

The objective of this research is to find planetary nebulae (PNe) and star cluster associations in the Andromeda galaxy (M31). To identify PNe in M31, a red-green-blue image is obtained using 3 emission line filters of $H\alpha$, $\lambda 5007\text{\AA}$ [OIII], and $\lambda\lambda 6717, 6731\text{\AA}$ [SII], using images from the Local Group Survey. By completing a visual search of the RGB images, 477 PN candidates are identified. In order to find star clusters associated with the PN candidates, an RGB image is made using the Panchromatic Hubble Andromeda Treasury survey. Filter F814W is used as red and filter F475W is used as both the green and blue colors. Two PN/open cluster (OC) association candidates appear to be the best cases to focus on. In one of the cases, the PN candidates is not confirmed as a true PN. In the other case, the PN appears to be confirmed as a true PN and so there is a good chance that PN/OC association is true for this case.

CHAPTER 1

THE INTRODUCTION

1.1 Background

A planetary nebula (PN) is a gas cloud, often a spherical shell, ejected from the outer layers of an evolved star as its core is transforming into a white dwarf. Ultraviolet light from the core illuminates the shell of gas, which emits spectral lines through fluorescence. Planetary nebulae were first noted by William Herschel in the 1780s. They were seen as giant gas clouds of round shape just like planets. As a result he called them planetary nebulae. The caveat is that in modern times we have become aware that these are not planets, but this designation has stayed ever since [6].

The lifetime of a PN depends greatly on the mass of the host star, which must be between $0.8\text{--}8 M_{\odot}$, where M_{\odot} represents the mass of the Sun [12]. After exhausting their helium shell, stars with masses in that range will move to the Asymptotic Giant Branch (AGB). In the AGB, stars become unstable and start pulsating in and out, leading to the ejection of the outer layer. Then the naked carbon-core, which is still hot and dense, illuminates the gas clouds around it with ultraviolet rays which starts an ionization process in the gas cloud [6]. The ionized gas cloud will emit visible light through fluorescence that can be observed around the hidden white dwarf core of the PN.

We have gained more knowledge about PNe in the Milky Way Galaxy since the 1780s, but our knowledge of their properties has been limited, as we are observing them from within our own Galaxy. Accuracy of the study of Galactic PNe have been limited by discrepancies related to the uncertainties in the measure of distance. Since Open Clusters (OCs) have been well studied, these uncertainties can be reduced to as little as 10 percent of the PNe found in association with an OCs [8]. Detection of these associations is obstructed by numerous galactic factors: the first, according to Majaess et al. [8] is the crowded region around the galactic bulge where the majority of PNe candidates are located. The second is the short lifetime of the PNe which is strongly dependent on their initial mass or the mass lost during evolution. In addition, galactic

dust and gas interfere or block the light emitted from the PNe. For instance, to avoid potential spatial coincidence between PNe and OC, Bidin et al. [2] use radial velocities to confirm associations of PN/OC found by several other studies. They then also apply a field-star decontamination algorithm. This complex process seems to be the best way to confirm association of PN/OC with the least possible errors in our Galaxy. These limitations have held us back from solving the mystery of PNe relationships with star clusters. PNe come in different forms and have short life spans. Although the PN structural properties have been known to the scientific community, PNe sometimes surprise scientists by appearing in places that are least expected, such as stellar clusters.

1.2 Analyzing Stars With the Hertzsprung-Russell Diagram

Photons detected from distant stars provide us with valuable information which aids in studying stars. A useful diagnostic is the Hertzsprung-Russell (H-R) diagram which plots the luminosity against the surface temperature of a group of stars. H-R diagram was created by two independent scientists: in 1911 by Ejnar Hertzsprung, and in 1913 by Henry Norris Russell [11]. A useful but simpler version of the H-R diagram can be made by plotting stars' absolute magnitude against their "color index," which is the difference in magnitude between two filters. In this version, the color index substitutes for the temperature, since the hotter a star is, the bluer its color will be. These diagrams demonstrate that stars do not behave randomly but instead are found in distinct regions of temperature and luminosity. As a result, the evolution of stars can be mapped out. H-R diagrams can help us to estimate the age of a star, its initial and current masses, and the distance of the star from us.

How stars evolve through the H-R diagram, as shown in Figure 1.1, is mainly related to their mass. A young star begins its life in the main sequence, burning hydrogen. Most of the star's lifetime is spent in the main sequence phase. The higher a star's mass, the faster it burns its hydrogen layer. As a result, a high-mass star moves through the main sequence phase faster than lower mass stars. The very-upper-left area of the main sequence has the highest mass, temperature, and luminosity. The very-lower-right part of this region has the lowest mass, temperature, and luminosity. Our Sun, which is in its hydrogen-burning phase, can be located

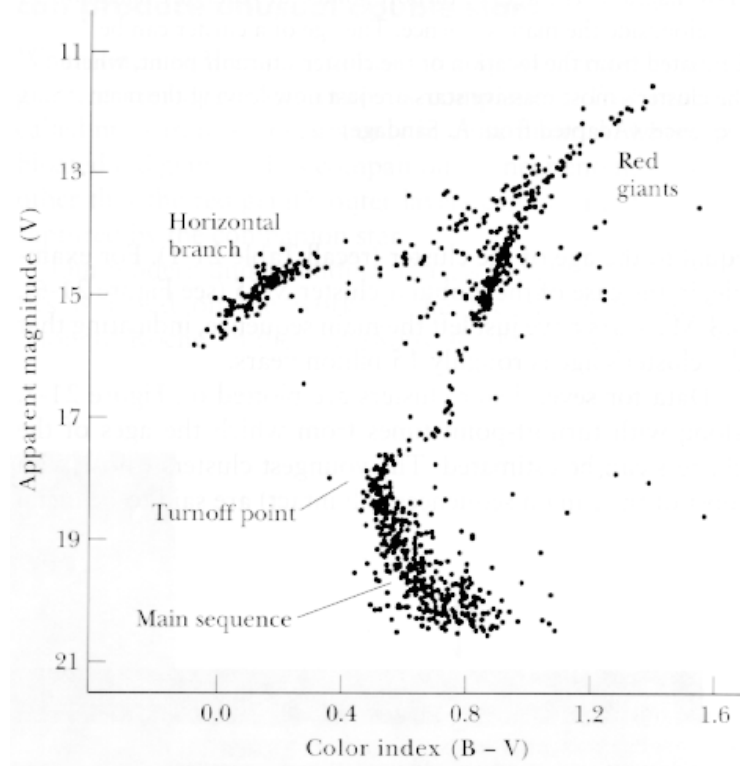


Figure 1.1 Hertzsprung-Russell diagram of a star cluster. Reproduced from [http://abyss.uoregon.edu/js/images/m13_hr.gif]

approximately in the middle of the main sequence branch.

1.3 Overview of Stellar Evolution

The interstellar medium is the gas and dust space between galaxies and star systems. When it clumps into clouds, they are known as interstellar clouds. Interstellar clouds are generally in a

peaceful harmony and equilibrium which makes it harder to get them fragmented into stars. Some sections of these clouds, called nebulae, are dense enough that they can become the birth place of stars and sometimes are illuminated through fluorescence. Nebulae are mostly made out of hydrogen and helium gases. When hot stars in nebulae emit strong ultraviolet light, hydrogen atoms may become ionized in the region. These regions are called the HII regions and can indicate where stars are being born. Strong stellar winds, explosions, or even gravitational forces of dense clouds can fragment clouds and make them collapse to form many new stars.

The collapsing cloud forms a core by the gravitational forces. The more the mass falls in, the more energy it releases, resulting in the rise of temperature. Over time, the dense core spins up through the conservation of angular momentum. A protostar is formed when this core turns opaque. When a protostar reaches at least $0.08 M_{\odot}$ and its temperature rises to more than 10^7 Kelvin (K), it is hot enough to start the nuclear fusion of hydrogen¹. Start of nuclear fusion in core changes a protostar into a star. Stars go through several stages of evolution from birth until their ends. Each stage in the life of a star strongly depends on its mass and the mass it has lost. The low-mass stars we are interested in here may go through the following stages in their lifetime: Main Sequence (MS), Red Giant Branch (RGB), Horizontal Branch (HB), Asymptotic Giant Branch (AGB), and a White Dwarf (WD) + Planetary Nebula (PN), etc. Some of these phases are mapped out on the H-R Diagram in Figure 1.2.

Since our focus is mainly on the planetary nebulae, it is important to know what a star goes through in its earlier stages before it becomes a planetary nebula and white dwarf. We can start by understanding the life of Sun-like stars. The main sequence of life of a star begins shortly after a protostar turns into a star. The star spends most of its life in the main sequence because it is burning hydrogen, which makes up most of the star's mass. As a star runs out of hydrogen in its core and fills it up with helium, the shell layer around the core has a high temperature. This temperature is enough for the hydrogen to continue burning into helium in the shell, causing the star to get swollen and brighter. As a result, the star will leave the main sequence and move up to a region of the H-R diagram called the Red Giant Branch [11].

For a star in a red giant branch, the amount of helium in its core continues to increase and

¹<https://lco.global/spacebook/protostar/>

become more dense as its hydrogen fusion is moving outward away from the core. At this point, the star is not hot enough yet for helium to fuse, so the newly created helium starts falling into the center because of its greater mass. As the helium core continues to grow, the temperature increases, although the pressure stays constant due to electron degeneracy. This rapid increase in temperature leads to a helium flash, which is the initiation of helium fusion. At this stage of a star's life, the core is fusing helium into carbon and small amounts of oxygen, while the surrounding shell is fusing hydrogen into helium. As a result, the star moves from the red giant branch onto the horizontal branch [11].

Stars in the horizontal branch have very similar luminosities, and they have a higher temperature than those in the red giant branch. The helium-burning process in the horizontal branch can take 100 million years. When all the helium in the core is used up, the core will contract and releases gravitational potential energy that heats the outer layer. Helium burning continues in a shell above the core, and hydrogen burning continues in a shell above that. During this stage of a star's life, the star will have two fusion shells and a C-O core. Now the star will move into asymptotic giant branch (AGB) [11].

Stars with more mass continue staying in the red giant or super giant branch until they run out of their current fuel and have enough heat to start fusion with a heavier element. But a lower-mass star becomes a white dwarf, which has no more fusion and only the residual thermal energy left over from its last fusion stage. A white dwarf will slowly cool down and darken [11].

1.4 Planetary Nebula Formation

During the AGB phase, stars continuously lose mass by thermal pulsations, stellar winds, and radiation pressure. Mass loss of stars in the AGB phase is so great that at times it can cause even higher-mass stars to lose enough mass to eventually form a PN. After years of mass loss (especially from the outer hydrogen layer of the star), the core does not have enough gravitational force to hold its layers tightly. As a result, the outer shells expand, leaving a gap between outer shells and the core of the star. The planetary nebula is formed when fast winds moving in the gap between the core and the outer shells push the outer shells into the universe while leaving the dense core behind [6]. The C-O core is still burning at high temperature. As a

result, it emits ultraviolet light that illuminates the gas envelope around it, leading to fluorescence that makes the gas clouds emit beautiful colors of visible light that can be observed by humans.

1.5 Associations Between Planetary Nebulae and Star Clusters

Stars are born in batches that are bound to each other gravitationally. These batches of stars are called star clusters and come in different types. Globular clusters (GCs) are highly dense and spherical, and host around 10^6 stars. Globular clusters are the oldest type of clusters. As a result they have the oldest stars within them, appearing overall red in color. They have no high-mass main sequence stars found in their H-R diagram. Importantly, they are not expected to host a PN since GCs are so old that the $0.8\text{--}8 M_{\odot}$ stars that form PNe should already have gone through the planetary nebula phase by now [7].

Lower-mass star clusters are called Open Clusters (OCs), and usually have 100s to 1000s of stars². They host younger stars and are blue in color. These clusters are not very stable gravitationally and usually survive between 10^8 years to a few billion years depending on their size, before they disperse into the galaxy. Most open clusters that are close to each other were created by the same regional disturbance, and as a result they have the same age. In addition, all stars in one cluster are created at the same time and have the same age. The age of a cluster can be determined by the aid of its H-R diagram. As the age of the cluster increases, the turning point of the main sequence stars moving to the giant branch changes. The turning point will increase in redness and become dimmer. Movement of turning point is caused by younger and more massive stars moving to the giant branch or other phases. Although OC host younger stars, still the short lifetime of the PN can affect the odds of finding a PN/OC association. Although, if an association is established, the PN's progenitor can be the same mass as the maximum stellar mass in OC [1].

1.6 Previous Searches for Planetary Nebula—Cluster Associations

Majaess et al. [8] examine Milky Way PNe seen in the directions of open clusters in order to establish an association between them. In case of a confirmed association, the authors calibrate

²<http://abyss.uoregon.edu/~js/ast122/lectures/lec15.html>

the properties of the PN as a member of the cluster. This study is confronted with many complications. One of the factors affecting the search for a PN/OC association is the Galactic bulge and the large number of stars populating the area. The crowded field of the Galactic bulge forces them to avoid the majority of PN candidates that are located there. To confirm suspected associations, the study considers criteria such as the difference in radial velocity and color excess between the PN and the cluster. It also considers the apparent size of the objects, their angular separation, and Galactic location. Although the authors are not able to confirm any absolute OC/PN associations, they are able to save some of the candidates from being ruled out. They conclude the need for further follow-up studies for a number of cases. They also conclude that “almost all potential cluster planetary nebulae lie in cluster coronal regions, typically surrounding open clusters.”

Bidin et al. [2] examine PN/OC associations. Their goal is to obtain fundamental information about the end state of intermediate-mass stars by studying Milky Way planetary nebulae in open clusters. To confirm PN/OC associations, the authors measure the radial velocity of PNe and OCs involved in a potential association. Only one out of four candidates is found to be a true association, while two others are rejected, and one doesn't have enough evidence to confirm it as an association. UBV photometry of the confirmed PN/OC association, cluster NCG 4463, resulted in finding the distance, age, and magnitude of the cluster. It is concluded by Bidin et al. [2], that NCC 4463 hosts a PN and a core-helium burning F type supergiant. Beside the potential problems caused by the unique properties of PNe, Bidin et al. [2] have to deal with Galactic problems such as dust and gas blocking their sights, as well as the big probability of chance alignments of PNe and OCs.

While most of the work has dealt with associations with open clusters, Bidin et al. [2] give a little hint about the possibility of finding PNe associated with globular clusters (GCs) and what it could mean for the process of making PNe. Since GCs are older than stars producing PNe, the only way that a PN can appear in a GC is by binary star interaction or the merger of two stars in the crowded field of a GC. In fact, Jacoby et al. [7] focus on PN/GC associations in M31. They hope that by confirming an association, they will be able to confirm either the binary interaction or stellar merger model. They use an $\lambda 5007\text{\AA}[\text{OIII}]$ spectroscopic survey of PNe in

M31 selected from those that appear to be in association with GCs. To establish a PN/GC association, they require the presence of PN emission lines. Then the emission lines have to have the expected ratio of [OIII] to $H\alpha$, and the velocity of the PN has to be consistent with being a member of the GC. Although this method is effective in finding PN/GC association candidates, confirming the association by measuring the velocity is not an easy task. The uncertainties obtained for velocities are high, and they need better resolution of luminosity, velocity, and emission. They find three PN/GC candidates in M31 that have possible associations, but better data are necessary to be able to confirm the association.

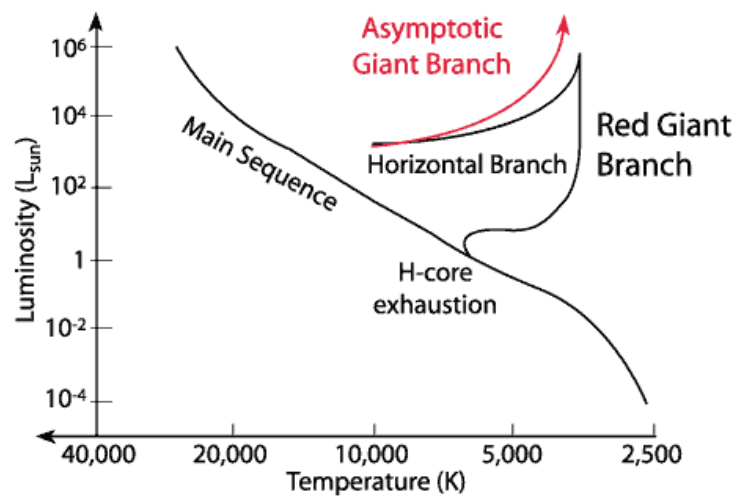


Figure 1.2 H-R diagram of PN progenitor star evolution. This diagram maps phases that a star will go through till it becomes a PN. Reproduced from Richard Pogge via [<http://aasnova.org/2016/07/26/mass-loss-in-dying-stars/>]

CHAPTER 2

DATA SETS

2.1 Local Group Survey

Local Group Survey (LGS)¹ focuses on understanding star formation and stellar evolution in UBVRI, $H\alpha$, $\lambda\lambda 6717, 6731\text{\AA}$ ([SII]), and $\lambda 5007\text{\AA}$ ([OIII]) filters. One of these galaxies is M3. Their emission-line images ($H\alpha$, [SII], and [OIII]) are of big assistance to me in this research. Using these emission line images I can identify PNe, just by looking through the images carefully. An overall image of M31 provided from LGS can be seen in Figure 2.1.

2.2 Panchromatic Hubble Andromeda Treasury

A large survey has recently been completed using the Hubble Space Telescope (HST) Multi-cycle Treasury Program to obtain a clear image of $\sim 1/3$ of the Andromeda galaxy's star forming disk in six filters, covering wavelengths from the ultraviolet (UV) to the near infrared (NIR). Image files were delivered online in 2014. This program is called the Panchromatic Hubble Andromeda Treasury² (PHAT) [4]. HST's high resolution and sensitivity makes it possible to study PNe in M31 in greater detail.

Studying PN/OC associations in the M31 galaxy has its advantages. One of the biggest advantages is the lack of a need to compute the distances of PNe, since all stars and nebulae within M31 are at nearly the same distance from Earth. In addition, because we are not viewing Andromeda edge-on, there is less dust obscuring the view, which helps us find and observe much bigger sample of PNe and get more accurate data than Galactic observations.

In PHAT survey publication IX, Veyette et al. [12] search for PNe using the $F336W$ (U), $F475W$ (B), and $F814W$ (I) broadband filters, rather than emission line filters. The nebulae's flux through the $F475W$ filter is mostly from the [OIII] emission lines. The authors are able to establish a linear relation between $\lambda 5007\text{\AA}$ ([OIII]) and $F475W$ PN magnitudes, as shown in Figure 2.2. Planetary nebulae appear to be distinguished by their bluish to green color in images

¹<http://www2.lowell.edu/users/massey/lgsurvey.html>

²<https://archive.stsci.edu/prepds/phat/>



Figure 2.1 Overall area of M31 covered by the Local Group Survey. Reproduced from [<http://www2.lowell.edu/users/massey/lgsurvey.html>]

made from $F336W$, $F475W$, and $F814W$ filters. In order for a candidate to be confirmed as a PN, it has to have a color $(F475W - F814W) \lesssim -1$.

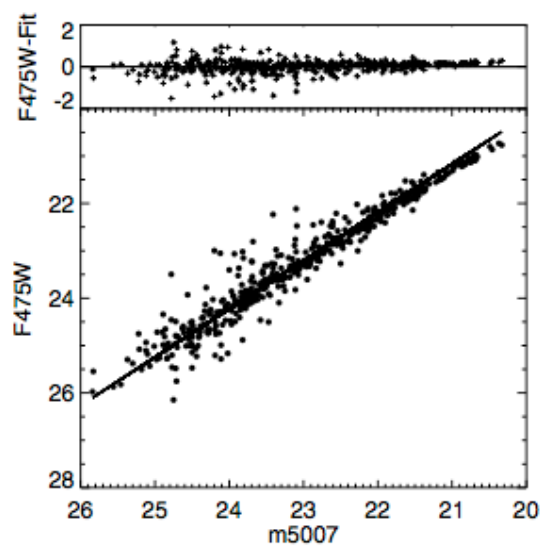


Figure 2.2 Linear relationship between m_{5007} and F475W magnitudes. Reproduced from [<http://iopscience.iop.org/article/10.1088/0004-637X/792/2/121>]

CHAPTER 3

Methods

3.1 Object Identification

3.1.1 Distinguishing PNe From Stars

In this study, I take advantage of emission lines that a PN has which distinguishes it from stars, hot dust, and other nebulae. PNe have very low gas density, allowing very rare electron transitions in atoms, emitting special emission lines known as “forbidden lines.” The lines we are interested in are produced by OIII, hydrogen, and SII ions. These emissions dominate the light from PNe [6]. After the identification process, only the PNe/OCs that appear to be associated are examined to obtain more detailed information.

In order to be able to distinguish PNe by their colors, I use images that have been taken with specific filters that can capture $H\alpha$, [OIII], and [SII] emission lines; unfortunately these data are not available in PHAT survey images. Luckily I am able to get my hands on images from the local group survey¹ done with the 4-m Mayall Telescope at Kitt Peak [9]. These Local Group Survey images cover the whole of M31 in 10 fields, but I only need the northeast side of M31, covered by fields 1 to 5, as can be seen in Figure 3.1. A wide-field camera is used in this survey to produce catalogs of *UBVRI* photometry for M31’s stars. By using the DS9² software, I make color images of M31. In an RGB frame, $H\alpha$ is used as red, [OIII] is used as green, and [SII] is used as blue (Table 3.1).

Since it is expected for a PN to have stronger [OIII] and [SII] emissions than $H\alpha$, they will appear greenish to brownish when the color image is made, while stars appear in white, blue, and red colors. Image filenames used from the Local Group Survey, the filters, and what color each filter was used for, are shown in Table 3.1.

Images of all fields are examined thoroughly, and the greenish to brownish objects are marked with DS9 regions (location markings) as PN candidates. By combining all the marked regions’

¹<http://www2.lowell.edu/users/massey/lgsurvey.html>

²<http://ds9.si.edu/site/Home.html>

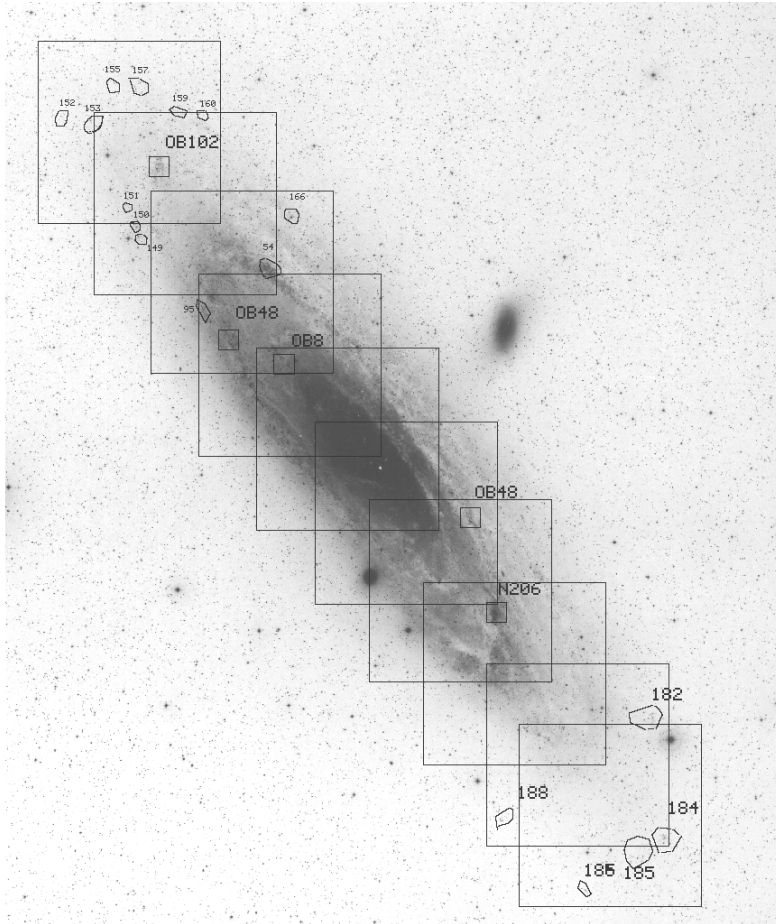


Figure 3.1 Area of M31 covered by the Local Group Survey images. Each field is specified with a number. Only fields 1, 2 ,3 ,4 and 5 are used for this research. Reproduced from [<http://www2.lowell.edu/users/massey/lgsurvey.html>]

positions, a catalog of all candidate PNe is made and saved as a DS9 region file. Since these fields overlay each other, some objects can be duplicated. To avoid having duplicated objects, it is important to load the region files made for the previous field first and then only mark PNe that haven't been marked; then save the region file again. This way by the time Field 5 is looked through, all the regions are in the same file, and there are no duplicates. This method is also effective to avoid small shifts of regions caused by coordinate shifts between images, if there are any. 478 PNe candidates are identified among all images. In Figure 3.2, the distribution of PNe candidates in 5 fields can be seen. The galactic bulge of M31 is located in Field 5. As it appears in Figure 3.2, most of the PNe candidates fall in fields 4 and 5, close to the galactic bulge.

Fields	Blue	Red	Green
1	M31F1HAm.fits	M31F1O3m.fits	M31F1S2m.fits
2	M31F2HAm.fits	M31F2O3m.fits	M31F2S2m.fits
3	M31F3HAm.fits	M31F3O3m.fits	M31F3S2m.fits
4	M31F4HAm.fits	M31F4O3m.fits	M31F4S2m.fits
5	M31F5HAm.fits	M31F5O3m.fits	M31F5S2m.fits

Table 3.1 **Local Group Survey Images Used in Making of Color Images**

3.1.2 Finding Stellar Clusters

Stellar clusters are identified from visual inspection of the PHAT survey images. The subject area of M31 is divided in 23 smaller “bricks” (Figure 3.3), and each of the bricks is then broken into 18 smaller sections named fields. I use Wide Field Camera (WFC) images of F475W (B) and F814W (I) filters for each field to create a RGB color image. F814W filter is used for the red channel and F475W filter is used for both green and blue.

Using the region file of PNe made from LGS images, I locate each PN and identify the nearest cluster. Since these images overlay each other in some parts, there could be some duplicated PNe. To avoid duplications, I go through the list and remove the duplicated coordinates. The information recorded for PNe and clusters, in Table A.1 and Table A.2 Appendix A, consists of PN coordinates (in sexagesimal notation), coordinates of the nearest cluster to each PNe (in sexagesimal), type and color of each cluster, distance of each PN to the cluster (in arcsec), and descriptions if there is pertinent observational information. The distance of each PN to its nearest cluster is measured to the center of the cluster by using a Ds9 ruler region. If there are no clusters closer than edge of the image to PN, then the distance to the edge is recorded.

Table 3.2 lists the images used from the PHAT survey. To understand the filenames, take the following example: “hlsp_phat_hst_acs-wfc-12058-m31-b01_f475w_v1_drz.fits” is an example of an astronomically-corrected, drizzled image. ‘HST’ (Hubble Space Telescope) is the name of the telescope used to acquire data. ‘ACS’ (Advanced Camera for Surveys) is the identifier for the instrument used to acquire data. ‘WFC’ stands for the wide field camera setting. 12058 is the proposal identifier. ‘m31-b01_f475w’ is the proposer’s target name that consists of galaxy-brick-filter. Each brick is divided into 18 fields in case smaller files are needed. For smaller images the target name will consist of ‘m31-*brick* - *field*.f475w’. To distinguish between

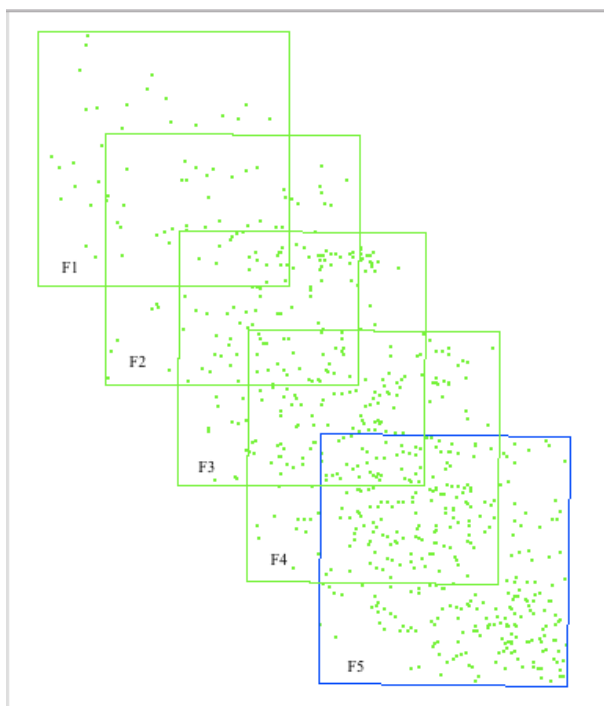


Figure 3.2 PN candidate distribution in M31. Green or blue squares show the outline of fields 1 to 5 of LGS images (there is no particular reason for the blue square). Green dots show the candidate PNe through the fields. Refer to Figure 3.1 for the locations of the fields within M31.

images for each filter, I refer to its target name which specifies brick, field, and the filter.

3.2 Photometry

Photometry is performed on candidate planetary nebulae using the PyRAF software package Digiphot. The software tasks are run as noted below:

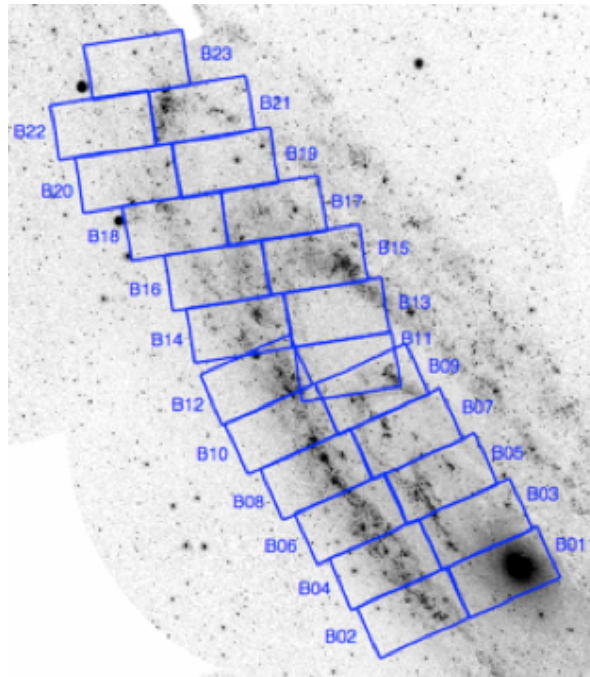


Figure 3.3 PHAT survey layout of the 23 image bricks on M31. Reproduced from [<https://archive.stsci.edu/prepds/phat/datalist.html>]

1. Digiphot — This is the package that includes the following tasks (programs)
2. Daophot — Crowded-field photometry package
3. Daoedit — For measuring the image statistics
 - Prior to running this step, a DS9 window is opened in another terminal tab to avoid display errors.
 - To have a more accurate result it is advised to choose both dim and bright stars that are as segregated as possible.
 - At least 5 stars are chosen and the average of their parameters is recorded to be used for the next steps.
4. Datapars — For editing the Daophot parameter sets
 - Most of the parameters needed in these steps are obtained from the header files of the images.
 - The parameter Datamin has to be calculated: $\text{Datamin} = \text{Sky} - 5 \times (\text{Sky sigma})$
5. Daofind — Identifies the stars in the image
 - This step is only used to generate a list of stars and their coordinates. This step is skipped when I already have a coordinate list.
6. Phot — Compute sky values and initial magnitudes for a list of stars
 - Prior to running the Phot command, the parameters given to Photpars, Centerpars, Fitskypars should be checked and corrected if needed.

The output of Phot provides intensity in units of counts. To convert this count, F_c (counts), into flux, F (ergs/sec/cm²/Å), for the Local Group Survey images, the following conversion factors are to be multiplied by the count:

- H α : 1.79E-16
- [SII]: 1.84E-16

- [OIII]: 3.92E-16

But simply multiplying the conversion factors by my measured flux counts didn't provide the correct results. I determined that the exposure time of 300 seconds for each image must be accounted for as follows:

$$\frac{F_c \times 3.92 \times 10^{-16}}{300} = F_{5007}, \quad (3.1)$$

where F_{5007} is $\lambda 5007\text{\AA}$ [OIII] flux, the conversion factor is in the numerator, and the exposure time of 300 seconds is in the denominator. The other filter count rates are converted in a similar way, but using their individual conversion factor for their specific wavelength.

From the narrow-band $\lambda 5007\text{\AA}$ [OIII] fluxes, I obtain the corresponding m_{5007} magnitudes using the relationship given by Jacoby (1989),

$$m_{5007} = -2.5 \log(F_{5007}) - 13.74. \quad (3.2)$$

For the star clusters, my original plan was to do photometry of the PHAT images in the same way, using Phot. But Phot output for these images turned out to be suspiciously faint and had very high uncertainty. Luckily the photometry catalog of M31 [13] (their Table 5) is accessible through the Vizier catalogue services³. To obtain the photometry of an M31 cluster from Vizier, enter the max and min of RA and DEC coordinates of the cluster area and the center of the "target." In this case, the target is M31 itself, and its center must be specified in the target name field in J2000 RA+Dec format.

3.2.1 F475W-[OIII] magnitude relation

Using the Figure 2.2, I obtained the formula,

$$m_{F475W} = (1.034 \times m_{5007}) - 0.575 \quad (3.3)$$

³<http://vizier.cfa.harvard.edu/viz-bin/VizieR-3?-source=J/ApJS/215/9/table5>

which shows the relation between F475W magnitude and $\lambda 5007\text{\AA}[\text{OIII}]$ magnitude. Using this relation I can calculate the expected F475W magnitude for a PN with a given [OIII] magnitude. Using the calculated F475 magnitude, I am able to distinguish and examine the PN candidate in a H-R diagram.

3.2.2 Chance Alignments

One of the important benefits of looking at PN/OC associations in M31 is that unlike in the Milky Way Galaxy, we are not looking at it edge-on, which means that the chance of random alignments is reduced and there is less dust along the line of sight. The probability of PN/OC overlapping is calculated using formulas below:

$$\frac{(\text{Number of clusters}) \times (\text{Average area of an open cluster})}{\text{Area of survey}} = P_1 , \quad (3.4)$$

where P_1 is the probability of one PN aligning with one open cluster. The possibility of one coincidental alignment is $(1 - P_1)$. In order to calculate the coincidental alignments probability for a number of PNe, this formula is used:

$$(1 - P_1)^{N_{PN}} = \text{Probability of any PN overlapping an OC} , \quad (3.5)$$

where N_{PN} is the number of PNe found in the survey area. The details of these calculations are discussed in Section 4.

Field	Image filenames
1	hlsp_phat_hst_acs-wfc_12058-m31-b01_f475w_v1_drz.fits hlsp_phat_hst_acs-wfc_12058-m31-b01_f814w_v1_drz.fits
2	hlsp_phat_hst_acs-wfc_12073-m31-b02_f475w_v1_drz.fits hlsp_phat_hst_acs-wfc_12073-m31-b02_f814w_v1_drz.fits
3	hlsp_phat_hst_acs-wfc_12073-m31-b03_f475w_v1_drz.fits hlsp_phat_hst_acs-wfc_12073-m31-b03_f814w_v1_drz.fits
4	hlsp_phat_hst_acs-wfc_12073-m31-b04_f475w_v1_drz.fits hlsp_phat_hst_acs-wfc_12073-m31-b04_f814w_v1_drz.fits
5	hlsp_phat_hst_acs-wfc_12073-m31-b05_f475w_v1_drz.fits hlsp_phat_hst_acs-wfc_12073-m31-b05_f814w_v1_drz.fits
6	hlsp_phat_hst_acs-wfc_12073-m31-b06_f475w_v1_drz.fits hlsp_phat_hst_acs-wfc_12073-m31-b06_f814w_v1_drz.fits
7	hlsp_phat_hst_acs-wfc_12073-m31-b07_f475w_v1_drz.fits hlsp_phat_hst_acs-wfc_12073-m31-b07_f814w_v1_drz.fits
8	hlsp_phat_hst_acs-wfc_12073-m31-b08_f475w_v1_drz.fits hlsp_phat_hst_acs-wfc_12073-m31-b08_f814w_v1_drz.fits
9	hlsp_phat_hst_acs-wfc_12073-m31-b09_f475w_v1_drz.fits hlsp_phat_hst_acs-wfc_12073-m31-b09_f814w_v1_drz.fits
10	hlsp_phat_hst_acs-wfc_12073-m31-b10_f475w_v1_drz.fits hlsp_phat_hst_acs-wfc_12073-m31-b10_f814w_v1_drz.fits
11	hlsp_phat_hst_acs-wfc_12073-m31-b11_f475w_v1_drz.fits hlsp_phat_hst_acs-wfc_12073-m31-b11_f814w_v1_drz.fits
12	hlsp_phat_hst_acs-wfc_12073-m31-b12_f475w_v1_drz.fits hlsp_phat_hst_acs-wfc_12073-m31-b12_f814w_v1_drz.fits
13	hlsp_phat_hst_acs-wfc_12073-m31-b13_f475w_v1_drz.fits hlsp_phat_hst_acs-wfc_12073-m31-b13_f814w_v1_drz.fits
14	hlsp_phat_hst_acs-wfc_12073-m31-b14_f475w_v1_drz.fits hlsp_phat_hst_acs-wfc_12073-m31-b14_f814w_v1_drz.fits
15	hlsp_phat_hst_acs-wfc_12073-m31-b15_f475w_v1_drz.fits hlsp_phat_hst_acs-wfc_12073-m31-b15_f814w_v1_drz.fits
16	hlsp_phat_hst_acs-wfc_12073-m31-b16_f475w_v1_drz.fits hlsp_phat_hst_acs-wfc_12073-m31-b16_f814w_v1_drz.fits
17	hlsp_phat_hst_acs-wfc_12073-m31-b17_f475w_v1_drz.fits hlsp_phat_hst_acs-wfc_12073-m31-b17_f814w_v1_drz.fits
18	hlsp_phat_hst_acs-wfc_12073-m31-b18_f475w_v1_drz.fits hlsp_phat_hst_acs-wfc_12073-m31-b18_f814w_v1_drz.fits
19	hlsp_phat_hst_acs-wfc_12073-m31-b19_f475w_v1_drz.fits hlsp_phat_hst_acs-wfc_12073-m31-b19_f814w_v1_drz.fits
20	hlsp_phat_hst_acs-wfc_12073-m31-b20_f475w_v1_drz.fits hlsp_phat_hst_acs-wfc_12073-m31-b20_f814w_v1_drz.fits
21	hlsp_phat_hst_acs-wfc_12073-m31-b21_f475w_v1_drz.fits hlsp_phat_hst_acs-wfc_12073-m31-b21_f814w_v1_drz.fits
22	hlsp_phat_hst_acs-wfc_12073-m31-b22_f475w_v1_drz.fits hlsp_phat_hst_acs-wfc_12073-m31-b22_f814w_v1_drz.fits
23	hlsp_phat_hst_acs-wfc_12073-m31-b23_f475w_v1_drz.fits hlsp_phat_hst_acs-wfc_12073-m31-b23_f814w_v1_drz.fits

Table 3.2 PHAT Survey Images Used to Find PN/OC Association Candidates²²
These image files consume lots of space. Each Image is also offered in 18 smaller files.

CHAPTER 4

RESULTS

601 clusters were found in 6 bricks, B1, B9, B15, B17, B21 and B23 by the PHAT survey team [5]. I have found 97 PNe in these 6 bricks. Each brick has a surface area of 390 arcmin^2 . The average radius of several randomly chosen clusters is calculated to be 1.4 arcsec , which gives an area of 6.17 arcsec^2 . The outline of open clusters is measured from the visual outline of the denser region at the core of the cluster. Clusters can have an extended, less obvious corona that is about 2.5 to 10 times larger than the radius of the core region that is easily visible [8]. With these numbers, the probability of a PN and the nucleus of an open cluster overlapping by chance in M31 is 0.77%, using formulas 3 and 4. This probability gives me a good confidence in the detected associations. A list of my PN/OC association candidates is in Table 4.1.

ID	(PHAT) Code	Coordinates (RA, Dec)
457	6-9-1	11.13087741 , 41.35871628
609	2-9-1	10.954454 , 41.160778

Table 4.1 **PN/OC Association Candidates.** ID is the identification number from Table B.1 in Appendix B. Coordinates are in degrees. (PHAT) code is from Table A.1 in Appendix A. PHAT code specifies brick-field-PNnumber.

4.1 Planetary Nebula Luminosity Function

The planetary nebula luminosity function for PN candidates is created using the photometry data in Table B.1 in Appendix B, by plotting the number of PNe vs. apparent magnitude of [OIII] emission (Figure 4.1, Figure 4.3). By comparing with the results of Ciardullo et al. [3](Figure 4.2, Figure 4.4), I find that the luminosity function of my PN candidates closely matches theirs, giving evidence that my approach is generally finding actual PNe.

4.2 PN 609

The first PN/OC association candidate that is notable is PN 609, which has a separation of 0.63 arcsec from a small open cluster and seems to be within it. This PN is only distinguishable in LGS emission-line filters. In the PHAT broadband F475W filter, the dim and small open

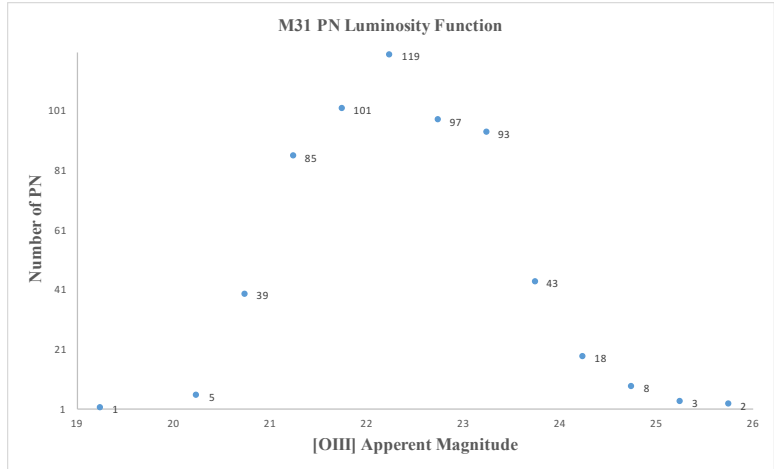


Figure 4.1 The luminosity function of the PNe candidate catalog. M31 luminosity function of PNe found and detected in the photometry process. This plot is compared to the module plot shown in Figure 4.2.

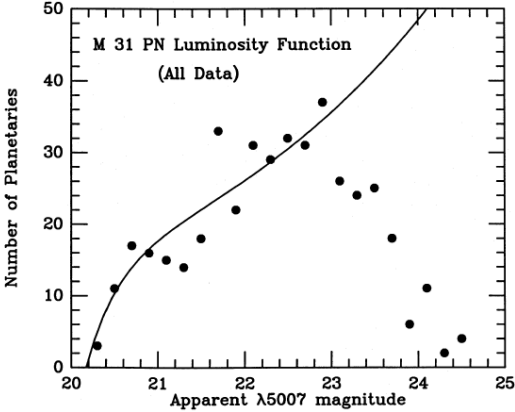


Figure 4.2 The luminosity function of PNe module. The luminosity function of PNe presented by Ciardullo et al. [3]

cluster can be seen (see Figure 4.5). In the RGB images I made using F475W and F814W filters of PHAT survey, planetary nebulae tend to be bluish in color, just like the cluster, making

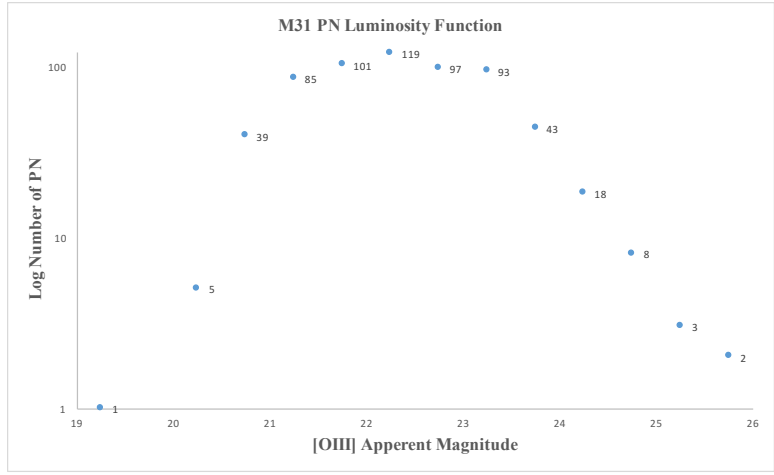


Figure 4.3 The logarithmic luminosity function of PNe candidate catalog. M31 logarithmic luminosity function of PNe found and detected in the photometry process. This plot is compared to the module plot shown in Figure 4.4.

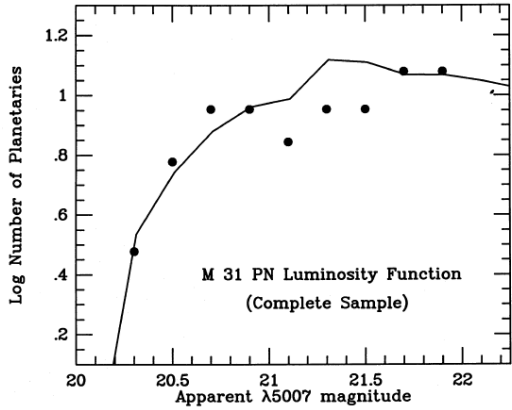


Figure 4.4 The logarithmic luminosity function of PNe module. The logarithmic luminosity function of PNe presented by Ciardullo et al. [3]

identification of the PN with a particular source difficult.

In order to test if PN 609 is a true planetary nebula and to identify it in the PHAT image of

the cluster, I create a color-mag diagram of the cluster region using PHAT photometry data from Vizier. The color-magnitude diagram of this cluster is shown in Figure 4.7. Using the expected F475W magnitude= 22.99, I was able to narrow it down to 3 objects that could be PN 609 from all the stars in the OC. There are two conditions for an object to meet to be identified as PN 609: First it should have a F475W magnitude close to the expected value. Second, it should have a color $(F475W-F814W) < -1$. None of the objects marked in Figure 4.8 and Figure 4.9 have the right color to be confirmed as a true PN.

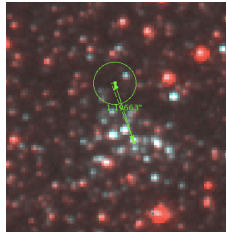


Figure 4.5 PHAT view broad-band of PN609 and its cluster. A blue open cluster appears to be located very close to one of the PN regions that was marked using the [OIII] filter. Since PN color appears blue in the broad band images, it is not easy to distinguish the PN. Coordinate mismatches between LGS and PHAT images means the PN's exact location can vary from the mark.

Parameters for PN609 are shown in Table 4.2.

ID	RA	DEC	Flux(counts)	Flux (ergs/sec/cm ² /Å)	[OIII] mag	F475W - mag
609	10.95435516	41.16085771	1868.953	2.4421E-15	22.79	22.99

Table 4.2 PN609 Parameters.

4.3 PN 457

A second notable PN/OC association candidate is PN 457, which appears to be 0.8 arc sec away from a clump of blue stars, which could be a smaller OC, and also around 5 arcsec away from a bigger OC. An image of this PN taken by LGS is shown in Figure 4.10. PN 457 and the

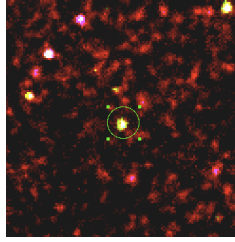


Figure 4.6 LGS emission-line view of PN 609. Green circle marks PN 609.

clusters around it are shown in Figure 4.11 using PHAT survey images.

To confirm this candidate I created the color-mag diagram shown in Figure 4.12, using the same approach as for PN 609. Only one object with the right color appears in close proximity to the expected magnitude $F475W=21.27$. This object meets both conditions to be approved as a PN.

Parameters for PN 457 are shown in Table 4.3.

ID	RA	DEC	Flux(count)	Flux (ergs/sec/cm ² /Å)	[OIII] mag	F475W - mag
457	11.13077076	41.35884425	9074.191	1.18569E-14	21.1275884	21.27

Table 4.3 PN457 Parameters.

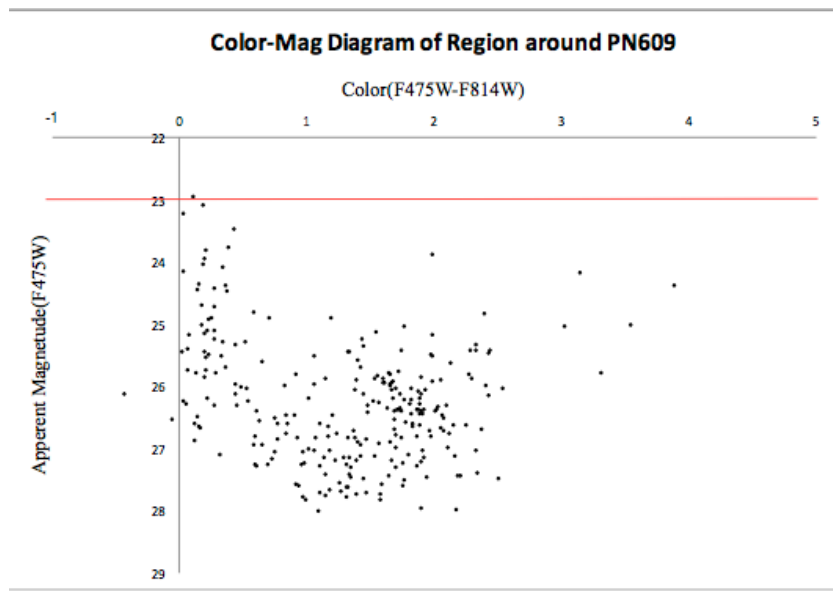


Figure 4.7 Color-mag diagram of region around PN 609. The red line indicates the expected magnitude for PN 609 to have in F475W filter, if it is a PN. Three sources have the right magnitude but are not blue enough in color.

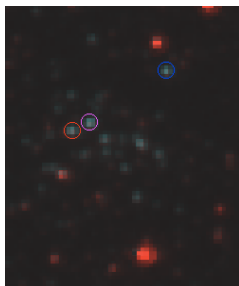


Figure 4.8 PN 609 and cluster. This image shows the PHAT RGB image of the cluster with the three candidate sources (noted in Figure 4.7) circled. Source marked with a blue circle is ruled out as being PN609 since its location has too big of a shift. PN 609 can be either sources with pink or red circles.

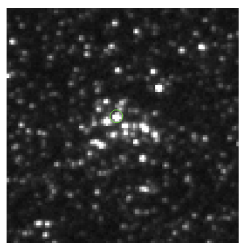


Figure 4.9 PN 609 and cluster in F475W filter of PHAT image. This image shows the F475W image of PN 609 and cluster, with the green circle marking the source that is closest in magnitude to the expected magnitude of 22.99.

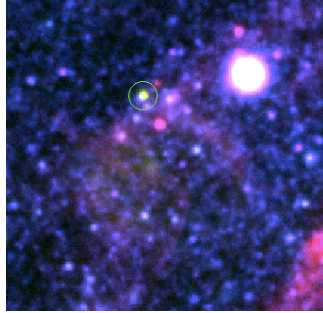


Figure 4.10 PN 457 in LGS images. This image shows the LGS image, with PN457 marked by a green circle. A GC is visible to the right, but the OCs cannot be seen.

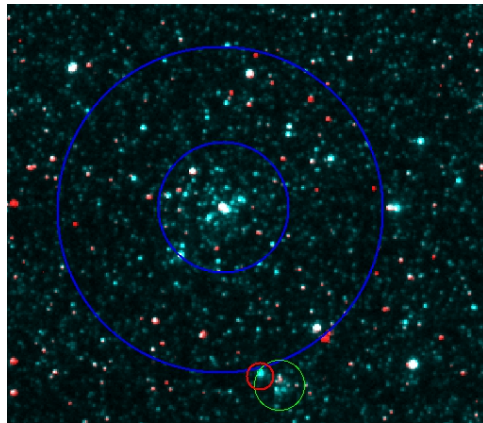


Figure 4.11 PN 457 and clusters in PHAT images. This image shows the PHAT image view of PN 457 (red circle), surrounded by a small OC (green circle) and the bigger OC (blue circle). The big OC is marked by two blue circles which shows the nucleus (inner circle) and the lower estimate of the corona radius (outer circle). The scale of the LGS image is wider than the PHAT image.

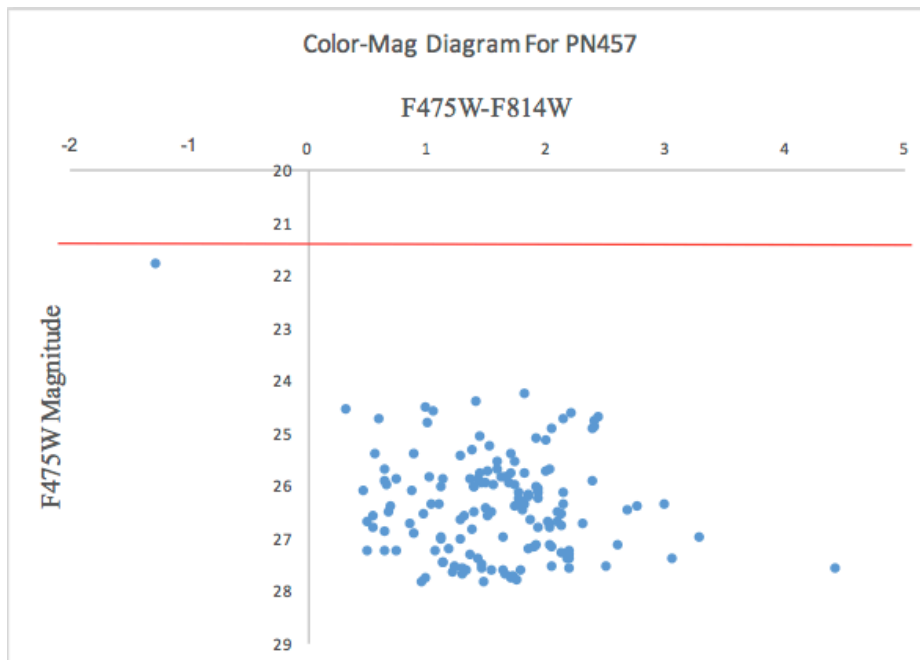


Figure 4.12 Color-mag diagram for PN 457. This diagram plots PN 457 and the smaller open cluster close to it. Red line indicates the expected PN of $m_{F475W} = 21.27$. Only one source in the image has the correct magnitude and color.

CHAPTER 5

DISCUSSION AND CONCLUSION

5.1 Discussion

This research was started with the goal of identifying PN associations with globular clusters using visual identification. It was not possible to identify any GC/PN candidates because the LGS images do not have the angular resolution needed to distinguish objects in the crowded field of a GC. The only PN associations that are found are with open clusters. Since OCs are loosely bound, the boundary between the extended “corona” of the cluster and the stars outside the cluster is not very clear. So in this work, the focus is on candidates that are very close to or in the nucleus of the OC. As Majaess et al. [8] point out, the corona of an OC can spread out 2.5 to 10 times bigger than its more obvious nucleus. More follow-ups on candidates that appear to be close enough to be located in the corona of an OC can give us more PN/OC association opportunities.

Around 477 potential PNe using LGS images are found. From 477 potential PNe (Table A.1) only 417 (Table B.1) are detectable in the photometry process. Each PN in each of these two tables has its location listed by coordinates which can be used to identify it in either table. ID numbers in each table only belong to the individual table. The focus is on my potential PN/OC identifications in Table B.1 Appendix B.

To verify the PN finding method, a histogram of PN [OIII] magnitudes is used to show their luminosity function (Figure 4.1). According to Ciardullo et al. [3], this luminosity function shows the expected curvature for a group of PNe. This figure confirms that the search method in this project is generally effective in finding PNe. The fall-off at faint magnitudes is due to a selection bias against faint objects, and the search method is complete to a magnitude of 22.5. The bias against the faint objects is caused by low resolution of LGS images. If the Hubble Space Telescope would obtain emission line images in future, this will make identifying PNe using the same method more effective and can be useful in improving our knowledge of these objects.

Color images (RGB) made by LGS images appear to have very green backgrounds, especially

Fields 3 and 4. That is, the [OIII] images seem biased relative to $H\alpha$ and [SII]. This error can turn some faint blue stars or objects greenish. In order to avoid this error, lower and upper limits for the green color scale are adjusted along with the contrast of all the three colors, in a way to have less green in the background. For each individual object, some adjustments might be needed, especially with contrast, to better examine the color of the object against its surroundings. It is therefore not possible to offer a consistent setting of color, scale, and contrast.

Figure 3.2 shows the PNe candidates distribution I have found by visual search in part of M31. A big number of PNe candidates seem to be located around the galactic bulge of 31 and the farther from the bulge the less PNe candidates can be located. Comparing Figure 3.2 to Figure 5.1, it seems that the distribution of PNe candidates founded in this research does not agree by the distribution of OCs. Although Figure 5.1 only includes data for 6 bricks, it seems that number of OCs increases the farther the bricks are from the galactic bulge of M31.

5.1.1 PN 609

PN609 is not distinguishable from other stars in the crowded field of the cluster. Therefore, I believe that PN609 should be one of the blue objects in the OC. To confirm the PN/OC association, a color-mag diagram of the cluster is created, shown in Figure 4.7. The red line on the graph indicates the expected magnitude for PN609. Because of close proximity and small shifts in the coordinates, it is not possible to know exactly which of these three sources represents PN609.

Both sources marked by pink or red circles have similar magnitudes and are in close proximity. Neither one of these two sources has the color that is expected for a PN. According to Veyette et al. [12], a PN is expected to show as blue and around $(F475W - F814W) < -1$. Unfortunately, PN609 can not be confirmed as a true PN. As the result of this setback, this PN/OC association can not be confirmed.

5.1.2 PN 457

PN457 (Figure 4.10) appears to be located only 0.8 arcsec away from the center of a small clump of stars. The color-mag diagram for this PN and the clump of stars is shown in Figure 4.12. PN475 stands out from the other sources, with a magnitude $m_{F475W} = 21.81$ which

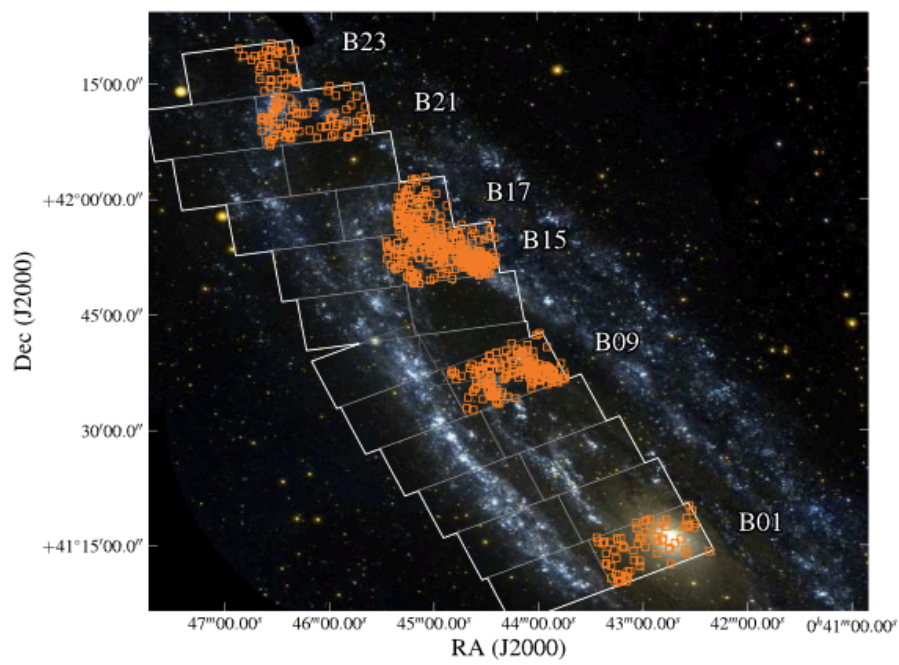


Figure 5.1 Distribution of open clusters in only 6 fields of M31. Reproduced from [5]

is very close to the expected value of 21.27. PN457 appear to have a color $(F475W - F814W) = -1.265$, which is what is expected for a PN. Candidate PN 457 appears to be confirmed as a true PN. A big OC can also be seen close to PN 457 in Figure 4.10. There is a good possibility that PN 475 can be located in the corona of this bigger OC. Majaess et al. [8] estimate a cluster's corona is 2.5 to 10 times bigger than what is visible of the nucleus of the cluster.

5.2 Future Work

PN and star cluster associations tend to be rare to find. Out of 477 PN candidates only two turn out to be located close enough to the nucleus of the OC to appear as an association, and one of these appears not to be a PN. It is expected that the corona of an OC is spread out 2.5 to 10 times bigger than its visible nucleus [8] and I have found around six or more candidates that are in close proximity to OCs but are not in their visible nucleus. I believe more follow up on these kind of PN/OC candidates can have a useful turn out.

5.3 Conclusions

In this research, I have investigated 2 PN/OC association candidates in M31 and at least one PN/OC association appears to be true. H-R diagram produced for PN609 candidate and its cluster (Figure 4.7) demonstrates that neither this candidate can be confirmed as a PN nor its association with the OC can be established. PN 609 does not appear as blue as a PN is expected to be, although it has the expected magnitude range. In the other case, the PN 457 candidate passes both tests of color and the expected magnitude according to its H-R diagram (Figure 4.12). As the result, the PN/OC association seems to be true for the PN 457 and its cluster.

In order to avoid all the troubles other scientists seem to be going through trying to find PN/OC associations, I have decided to take advantage of newly published PHAT survey images. By conducting a visual search of M31, using a RGB image produced from three emission line filters of $H\alpha$, [OIII] and [SII], from the LGS, I am able to find 477 PNe candidates. A luminosity function of all PNe candidates shows the reliability of my results for candidates as faint as $m_{5007}=22.5$. One of the advantages of searching for PNe in M31 is that the probability calculated

for a chance of overlay is only 0.77%. Star clusters associated with PN candidates are found by a visual search of an RGB image, made using the PHAT survey's filter F814W as red and filter F475W as both the green and blue colors.

I am optimistic about the methods I used in this research to find PN/OC associations in M31. The availability of better resolution emission line images can have a positive effect for my methods. An important advantage of this method is that since it uses archived images, it is both easily obtainable and affordable. One of the limitations in this research is the low angular resolution of emission line images. A lot of crowded star cluster members, such as stars in GCs, are not individually distinguishable. This limited my chances of finding any PN/GC associations. There is the possibility of human error in failing to see the PNe in the color images, but it can be reduced by re-checking the images.

Finding only one PN/OC association among 477 PN candidates means that the rate at which planetary nebulae are found in open clusters in the Andromeda galaxy is just 0.21 percent. There are at least 13 known PN/OC alignments [8] and about 3000 known PNe in the Milky Way Galaxy [10], giving an estimated alignment rate of 0.43 percent in our own Galaxy. However, Majaess et al. [8] reject seven of these alignments as coincidental. Taking this lower estimate of six alignments gives an alignment rate of 0.20 percent. This rate is comparable to what I have found for M31, but with the current data sets, I do not have a way of determining the coincidental alignments. Still the overall chance of a coincidental alignment is just 0.77 percent in M31.

APPENDIX A

LIST OF PN CANDIDATES FOUND IN M31

Table A.1. PN Candidate Coordinates

Brick	Field	PN	PN Coordinates ^a	Cluster Coordinates ^b
1	1	1	0:43:16.837 +41:15:13.57	0:43:18.205 +41:15:34.73
1	1	2	0:43:19.087 +41:15:09.25	0:43:18.205 +41:15:34.73
1	1	3	0:43:23.062 +41:15:40.57	0:43:25.600 +41:15:37.08
1	2	1	0:43:09.485 +41:15:52.70	0:43:12.449 +41:16:04.89
1	3	1	0:42:58.367 +41:17:09.56	0:42:58.128 +41:16:52.72
1	7	1	0:43:12.483 +41:12:43.71	No cluster
1	7	2	0:43:19.207 +41:12:12.67	0:43:18.135 +41:12:29.23
1	8	1	0:43:52.757 +41:12:31.54	No cluster
1	9	1	0:42:52.757 +41:14:15.34	0:45:51.641 +41:14:03.66
1	12	1	0:42:27.809 +41:16:31.17	0:42:29.935 +41:17:25.66
1	13	2	0:43:12.485 +41:12:43.71	No cluster
1	14	1	0:42:57.888 +41:12:42.52	No cluster
1	14	2	0:42:58.844 +41:12:49.55	No cluster
1	14	3	0:43:03.273 +41:12:10.99	0:43:01.586 +41:12:26.89
1	14	4	0:43:06.244 +41:10:55.41	0:43:09.232 +41:10:29.63
1	14	5	0:43:07.866 +41:12:31.54	0:43:07.185 +41:11:48.29
1	15	1	0:42:46.685 +41:13:15.30	No cluster
1	15	2	0:42:51.813 +41:12:14.36	0:42:51.642 +41:14:03.73
1	15	4	0:42:56.448 +41:13:28.95	0:42:51.642 +41:14:03.73
1	18	2	0:42:27.188 +41:14:34.24	No cluster
1	18	3	0:42:22.403 +41:16:04.01	No cluster
1	18	4	0:42:23.276 +41:13:36.35	No cluster
1	18	5	0:42:21.839 +41:14:10.66	0:42:18.658 +41:14:02.05
1	18	6	0:42:18.685 +41:15:56.39	No cluster
1	18	7	0:42:19.061 +41:14:03.24	0:42:18.657 +41:14:02.08
2	5	1	0:43:37.328 +41:14:29.90	0:43:37:304 +41:14:43.72
2	5	2	0:43:36.983 +41:15:09.32	0:43:37:304 +41:14:43.72
2	5	3	?	0:43:37:304 +41:14:43.72
2	6	1	0:43:28.579 +41:15:45.36	0:43:25.612 +41:15:37.06
2	6	2	0:43:23.049 +41:15:40.30	0:43:22.994 +41:15:25.47
2	8	1	0:44:07.508 +41:10:08.64	0:44:07.462 +41:09:43.36
2	8	2	0:44:04.892 +41:09:18.76	0:44:07.462 +41:09:43.36
2	9	1	0:43:48.973 +42:09:38.53	0:43:49.074 +41:09:38.61
2	9	3	0:43:55.155 +41:11:09.13	No cluster
2	9	4	0:43:58.860 +41:11:30.25	?
2	9	5	0:44:04.933 +41:09:18.35	?
2	10	2	0:43:48.971 +41:09:38.58	0:43:49.079 +41:09:38.59
2	10	3	0:43:43.225 +41:09:30.25	?
2	12	1	0:43:22.985 +41:10:50.59	No cluster
2	15	1	0:43:46.194 +41:10:50.59	0:43:45.497 +41:08:56.81
2	15	2	0:43:52.411 +41:09:06.07	0:43:53.570 +41:09:34.87
2	17	1	0:45:43.830 +41:59:33.53	No cluster
2	17	2	0:45:46.212 +41:59:41.92	0:45:45.827 +41:59:21.82
2	17	3	0:45:49.091 +41:59:37.91	0:45:47.827 +41:59:38.79
2	17	4	0:45:52.414 +42:02:12.05	0:45:53.925 +42:02:18.07
3	1	1	0:43:43.207 +41:20:21.80	0:43:43.368 +41:20:22.40
3	1	2	0:43:43.380 +41:19:34.86	No cluster
3	2	1	0:43:24.552 +41:22:04.11	0:43:25.996 +41:21:31.70

Table A.1 (cont'd)

Brick	Field	PN	PN Coordinates ^a	Cluster Coordinates ^b
3	2	2	0:43:23.245 +41:21:57.21	No cluster
3	2	4	0:43:28.413 +41:20:17.84	No cluster
3	3	1	0:43:23.245 +41:21:57.21	0:43:25.995 +41:21:31.69
3	3	2	0:43:24.564 +41:22:40.41	0:43:25.995 +41:21:31.69
3	3	3	0:43:23.423 +41:23:51.06	No cluster
3	3	4	0:43:24.543 +41:23:44.31	No cluster
3	3	5	0:43:24.224 +41:24:37.41	No cluster
3	4	1	0:43:13.192 +41:24:22.38	0:43:16.406 +41:24:04.56
3	4	2	0:43:60.951 +41:24:55.65	No cluster
3	5	2	0:42:58.309 +41:25:10.43	No cluster
3	5	3	0:42:57.552 +41:24:33.07	No cluster
3	6	3	0:42:49.199 +41:25:54.80	0:42:46.867 +41:26:20.35
3	7	1	0:43:32.750 +41:18:33.27	0:43:32.903 +41:18:14.72
3	7	2	0:43:34.380 +41:19:34.86	0:43:33.851 +41:19:42.66
3	7	3	0:43:41.395 +41:18:12.04	0:43:45.083 +41:18:12.12
3	7	4	0:43:43.602 +41:19:13.21	0:43:43.906 +41:19:42.33
3	8	2	0:43:26.656 +41:20:26.84	0:43:26.000 +41:21:31.69
3	8	3	0:43:28.314 +41:20:17.84	0:43:30.786 +41:21:16.41
3	9	1	0:43:08.797 +41:20:00.25	No cluster
3	9	2	0:43:12.573 +41:21:17.16	0:43:09.557 +41:21:32.20
3	9	3	0:43:18.049 +41:21:34.72	No cluster
3	10	2	0:43:08.804 +41:20:00.28	0:43:07.515 +41:20:19.77
3	11	1	0:42:58.844 +41:22:13.31	0:43:03.298 +41:21:21.67
3	11	2	0:42:57.424 +41:23:05.14	0:42:51.643 +41:23:29.92
3	11	3	0:42:56.646 +41:22:02.48	0:42:51.878 +41:22:05.19
3	11	4	0:42:54.516 +41:21:23.31	0:42:51.878 +41:22:05.19
3	12	1	0:42:51.646 +41:23:30.09	?
3	12	2	0:42:41.218 +41:24:22.10	0:42:39.786 +41:24:30.52
3	12	3	0:42:56.255 +41:22:02.48	No cluster
3	13	2	0:43:28.570 +41:15:45.40	0:43:25.610 +41:15:37.21
3	14	1	0:43:20.888 +41:17:51.92	0:43:26.239 +41:18:07.66
3	15	1	0:43:06.651 +41:18:37.65	0:43:08:009 +41:18:18.22
3	15	2	0:43:07.367 +41:19:21.93	0:43:09.849 +41:19:00.78
3	17	2	0:42:56.252 +41:22:02.48	No cluster
4	1	1	0:44:46.938 +41:15:28.21	0:44:44.826 +41:16:24.77
4	2	1	0:44:32.307 +41:17:45.60	0:44:32.691 +41:17:47.89
4	3	2	0:44:16:200 +41:18:53.13	0:44:16.414 +41:18:56.40
4	4	1	0:44:12.250 +41:20:40.4	No cluster
4	4	2	0:44:10.819 +41:18:14.01	0:44:10.606 +41:18:12.02
4	4	3	0:44:05.685 +41:18:02.58	0:44:07.745 +41:18:11.65
4	4	4	0:44:01.650 +41:19:38.21	0:43:59.885 +41:19:45.28
4	5	1	0:43:58.571 +41:19:23.43	0:43:59.874 +41:19:45.30
4	5	2	0:43:52.307 +41:18:51.47	0:43:52.492 +41:18:48.82
4	6	1	0:43:56.201 +41:22:13.04	0:43:56.426 +41:22:02.93
4	6	2	0:43:54.761 +41:22:04.52	0:43:54.386 +41:21:52.24
4	6	3	0:43:43.158 +41:20:22.20	0:43:43.368 +41:20:22.40
4	7	1	0:44:37.910 +41:14:14.10	0:44:40.240 +41:15:00.76
4	8	1	0:44:21.058 +41:15:39.52	0:44:20.112 +41:16:07.76

Table A.1 (cont'd)

Brick	Field	PN	PN Coordinates ^a	Cluster Coordinates ^b
4	10	2	0:43:59.483 +41:16:47.67	0:44:00.420 +41:16:25.28
4	10	3	0:43:59.889 +41:15:34.71	0:43:59.310 +41:15:26.88
4	12	2	0:43:41.359 +41:18:12.04	0:43:45.078 +41:18:12.08
4	14	3	0:44:14.045 +41:12:29.67	0:44:13.725 +41:13:18.16
4	14	4	0:44:11.912 +41:13:59.37	0:44:13.244 +41:13:30.64
4	15	1	0:44:04.566 +41:12:08.32	0:44:03.522 +41:12:47.36
4	15	2	0:44:09.411 +41:13:05.98	0:44:08.859 +41:13:14.02
4	15	3	0:44:10.792 +41:12:35.70	0:44:10.628 +41:13:07.95
4	17	1	0:43:43.513 +41:14:52.92	0:43:42.483 +41:14:50.58
4	18	2	0:43:36.949 +41:15:09.22	0:43:37.292 +41:14:43.45
4	18	3	0:43:37.328 +41:14:29.20	0:43:37.292 +41:14:43.45
5	1	1	0:43:58.808 +41:27:19.68	0:44:00.402 +41:27:16.91
5	1	2	0:44:02.615 +41:27:48.87	0:44:03.252 +41:27:48.87
5	1	4	0:44:06.882 +41:28:05.91	No cluster
5	2	3	0:43:58.812 +41:27:19.71	0:44:00.393 +41:27:16.91
5	3	2	0:43:41.596 +41:28:02.66	0:43:46.426 +41:27:24.93
5	3	5	0:43:49.541 +41:27:57.68	0:43:47.538 +41:27:07.96
5	4	1	0:43:42.032 +41:28:38.83	0:43:41.474 +41:28:27.98
5	4	3	0:43:39.681 +41:29:18.01	0:43:38.641 +41:29:47.06
5	4	5	0:43:28.298 +41:29:57.56	No cluster
5	5	1	0:43:28.389 +41:29:57.52	0:43:30.775 +41:29:26.34
5	5	2	0:43:27.860 +41:29:56.99	0:43:30.775 +41:29:26.34
5	5	3	0:43:26.226 +41:29:37.55	0:43:30.775 +41:29:26.34
5	5	4	0:43:23.871 +41:30:13.20	0:43:21.335 +41:30:40.60
5	5	5	0:43:24.207 +41:29:52.14	0:43:21.335 +41:30:40.60
5	5	6	0:43:20.417 +41:29:08.44	0:43:21.359 +41:29:16.86
5	5	7	0:43:17.430 +41:29:16.51	No cluster
5	5	8	0:43:14.594 +41:30:32.10	0:43:15.913 +41:30:32.95
5	6	5	0:43:11.123 +41:20:23.99	0:43:12.517 +41:30:48.69
5	6	6	0:43:06.182 +41:30:18.02	0:43:06.382 +41:30:27.73
5	9	1	0:43:37.979 +41:24:33.54	No cluster
5	9	2	0:43:39.234 +41:26:29.27	0:43:40.582 +41:25:50.12
5	9	3	0:43:41.596 +41:28:02.66	No cluster
5	11	1	0:34:24.207 +41:29:52.14	No cluster
5	11	2	0:43:26.896 +41:28:20.60	No cluster
5	11	3	0:43:20.410 +41:29:08.41	?
5	11	5	0:43:16.036 +41:27:03.94	0:43:17.634 +41:27:45.01
5	12	3	0:43:11.140 +41:30:24.02	No cluster
5	12	4	0:43:07.964 +41:28:25.16	0:43:07.373 +41:27:32.94
5	12	5	0:43:03.012 +41:29:24.54	No cluster
5	12	6	0:43:09.914 +41:27:06.62	No cluster
5	13	1	0:43:49.737 +41:22:42.32	0:43:46.681 +41:22:27.99
5	13	4	0:43:59.275 +41:21:48.23	0:43:57.996 +41:21:33.50
5	13	5	0:43:54.383 +41:23:33.09	0:43:52.952 +41:23:31.96
5	13	6	0:44:02.213 +41:22:50.62	No cluster
5	14	1	0:43:37.295 +41:22:37.63	0:43:38.772 +41:22:50.60
5	14	2	0:43:39.391 +41:22:57.32	0:43:38.772 +41:22:50.60
5	14	3	0:43:38.222 +41:24:05.37	0:43:35.899 +41:24:13.23

Table A.1 (cont'd)

Brick	Field	PN	PN Coordinates ^a	Cluster Coordinates ^b
5	14	5	0:43:49.725 +41:22:42.38	0:43:46.677 +41:22:28.11
5	15	6	0:43:37.976 +41:24:33.54	0:43:41.514 +41:24:25.47
5	17	1	0:43:16.086 +41:27:03.94	0:43:17.634 +41:27:45.01
5	17	2	0:43:16.663 +41:26:26.68	0:43:17.634 +41:27:45.01
5	17	5	0:43:10.750 +41:25:39.32	0:43:14.640 +41:25:13.44
5	17	7	0:43:06.951 +41:24:55.65	No cluster
5	18	2	0:43:07.964 +41:28:45.16	0:43:09.614 +41:27:06.62
5	18	4	0:43:10.748 +41:25:39.38	No cluster
5	18	5	0:42:58.671 +41:27:47.57	No cluster
5	18	6	0:42:56.858 +41:27:25.99	No cluster
6	1	1	0:44:56.301 +41:20:25.83	No cluster
6	1	2	0:44:06.708 +41:23:35.95	0:45:06.591 +41:23:18.74
6	4	1	0:44:32.206 +41:25:47.15	0:44:30.926 +41:26:01.63
6	4	2	0:44:27.078 +41:24:00.97	0:44:25.325 +41:24:12.19
6	4	4	0:44:27.491 +41:22:28.70	0:44:26.704 +41:22:41.35
6	5	1	0:44:25.585 +41:26:40.61	0:44:25.901 +41:26:30.06
6	5	2	0:44:23.893 +41:26:18.06	0:44:23.513 +41:26:15.93
6	5	3	0:44:23.725 +41:25:51.52	0:44:23.519 +41:26:16.00
6	5	5	0:44:20.846 +41:24:26.21	0:44:19.679 +41:24:08.82
6	6	1	0:44:15.623 +41:27:14.95	0:44:14.554 +41:27:42.78
6	6	2	0:44:13.471 +41:25:05.95	0:44:11.228 +41:25:22.69
6	6	5	0:44:07.404 +41:25:31.77	0:44:11.227 +41:25:22.70
6	7	1	0:44:56.308 +41:20:25.86	No cluster
6	9	1	0:44:31.407 +41:21:31.34	0:44:31.469 +41:21:30.85
6	10	2	0:44:28.345 +41:23:17.27	0:44:28.402 +41:23:27.48
6	11	3	0:44:16.853 +41:21:43.35	0:44:17.412 +41:21:43.57
6	11	4	0:44:15.909 +41:22:10.74	0:44:13.933 +41:22:18.82
6	11	5	0:44:13.633 +41:23:32.17	0:44:11.706 +41:23:53.96
6	12	3	0:44:05.255 +41:23:10.35	0:44:05.844 +41:23:17.83
6	12	4	0:44:02.212 +41:22:50.65	0:44:02.998 +41:22:44.06
6	13	2	0:44:53.080 +41:15:58.15	No cluster
6	13	3	0:44:46.991 +41:18:00.62	0:44:50.093 +41:17:48.82
6	13	4	0:44:50.698 +41:17:21.18	0:44:50.093 +41:17:48.82
6	16	1	0:44:16.200 +41:18:53.13	0:44:16.402 +41:18:56.40
6	17	1	0:44:15.902 +41:22:10.74	0:44:13.933 +41:22:18.82
6	17	3	0:44:12.250 +41:20:40.04	0:44:13.570 +41:21:20.24
6	18	2	0:44:02.219 +41:22:50.65	0:44:03.002 +41:22:43.98
7	1	1	0:44:24.946 +41:31:45.98	0:44:25.643 +41:31:31.88
7	1	2	0:44:26.245 +41:33:14.49	0:44:25.874 +41:33:29.21
7	1	3	0:44:29.796 +41:32:45.20	0:44:28.297 +41:32:57.67
7	2	1	0:44:09.563 +41:32:14.01	0:44:09.244 +41:32:28.20
7	2	2	0:44:11.000 +41:31:46.43	0:44:10.804 +41:32:02.56
7	2	3	0:44:13.502 +41:31:53.92	0:44:12.055 +41:31:53.26
7	2	4	0:44:15.098 +41:32:28.97	0:44:14.146 +41:33:18.74
7	2	5	0:44:17.642 +41:33:42.87	0:44:18.143 +41:34:03.93
7	3	2	0:44:04.661 +41:34:31.84	0:44:07.322 +41:33:53.01
7	3	4	0:44:11.300 +41:34:24.10	0:44:11.348 +41:34:21.40
7	4	2	0:43:54.776 +41:35:02.83	0:43:57.887 +41:34:57.27

Table A.1 (cont'd)

Brick	Field	PN	PN Coordinates ^a	Cluster Coordinates ^b
7	4	3	0:43:49.293 +41:35:31.55	0:43:47.750 +41:35:25.57
7	5	2	0:43:51.322 +41:36:21.20	0:43:52.192 +41:36:22.53
7	5	4	0:43:45.200 +41:35:17.57	0:43:45.217 +41:35:25.30
7	5	5	0:43:50.151 +41:36:01.38	0:43:38.202 +41:36:24.18
7	5	7	0:43:39.997 +41:35:03.72	0:43:38.873 +41:35:17.18
7	5	8	0:43:36.487 +41:35:49.66	No cluster
7	6	2	0:43:40.001 +41:35:03.60	0:43:38.872 +41:35:17.16
7	6	3	0:43:36.491 +41:35:49.54	0:43:36.617 +41:36:02.34
7	6	4	0:43:31.321 +41:37:27.32	No cluster
7	7	1	0:44:17.150 +41:29:48.26	0:44:18.773 +41:29:39.34
7	7	2	0:44:23.312 +41:29:32.89	0:44:27.100 +41:28:49.9
7	7	5	0:44:25.515 +41:29:53.37	0:44:24.989 +41:30:32.25
7	8	1	0:44:06.435 +41:32:03.29	0:44:06.384 +41:31:43.66
7	8	2	0:44:08.150 +41:31:18.94	0:44:06.384 +41:31:43.66
7	8	5	0:44:13.262 +41:30:09.98	No cluster
7	10	1	0:43:50.740 +41:32:51.15	0:43:55.815 +41:32:35.13
7	10	2	0:43:48.180 +41:31:26.41	0:43:50.102 +41:31:52.70
7	11	3	0:44:16.863 +41:21:43.39	0:44:17.396 +41:21:43.56
7	11	6	0:44:10.364 +41:24:17.53	0:44:10.595 +41:23:51.09
7	12	2	0:43:36.489 +41:35:49.59	0:43:36.620 +41:36:02.33
7	12	3	0:43:36.550 +41:33:02.68	0:43:37.814 +41:33:22.46
7	13	2	0:44:09.714 +41:27:12.42	No cluster
7	13	3	0:44:15.627 +41:27:14.83	No cluster
7	14	1	0:44:02.611 +41:28:03.88	0:44:03.234 +41:27:48.92
7	14	2	0:44:06.891 +41:28:05.95	0:44:05.069 +41:27:57.37
7	15	1	0:43:53.078 +41:27:57.08	0:43:51.447 +41:27:35.05
7	16	3	0:43:43.536 +41:30:57.32	0:43:39.361 +41:31:18.46
7	17	1	0:43:44.717 +41:31:18.37	No cluster
7	17	3	0:43:39.528 +41:32:09.73	0:43:39.365 +41:31:18.49
7	17	4	0:43:37.191 +41:31:04.42	0:43:39.365 +41:31:18.49
7	18	1	0:43:26.398 +41:31:44.99	0:43:29.070 +41:31:31.03
7	18	3	0:43:16.395 +41:32:59.52	No cluster
8	4	1	0:45:01.478 +41:30:18.99	0:45:01.854 +41:29:48.89
8	4	2	0:44:50.129 +41:31:08.73	0:44:50.106 +41:31:09.19
8	5	1	0:44:50.299 +41:31:50.34	0:44:50.506 +41:31:56.06
8	5	3	0:44:45.240 +41:31:48.92	0:44:46.221 +41:31:32.04
8	6	1	0:44:41.783 +41:32:04.20	No cluster
8	6	2	0:44:38.838 +41:31:31.39	0:44:38.883 +41:31:46.49
8	7	1	0:45:13.560 +41:24:04.79	0:45:14.119 +41:24:14.54
8	8	2	0:45:07.384 +41:25:28.22	0:45:07.127 +41:25:47.49
8	8	3	0:45:12.106 +41:25:29.84	0:45:07.127 +41:25:47.49
8	9	1	0:44:57.098 +41:26:16.59	0:44:59.421 +41:26:15.10
8	9	2	0:45:02.958 +41:25:26.27	No cluster
8	11	2	0:44:37.409 +41:27:09.15	0:44:37.245 +41:27:08.09
8	12	1	0:44:34.587 +41:29:16.30	0:44:37.854 +41:28:52.31
8	12	3	0:44:24.503 +41:29:46.93	0:44:27.068 +41:28:49.95
8	13	1	0:45:06.708 +41:23:35.95	0:45:07.203 +41:23:47.18
8	13	2	0:45:13.553 +41:24:04.76	0:45:14.111 +41:24:14.36

Table A.1 (cont'd)

Brick	Field	PN	PN Coordinates ^a	Cluster Coordinates ^b
8	14	2	0:45:02.958 +41:25:26.77	No cluster
8	17	1	0:44:37.404 +41:27:09.29	0:44:37.255 +41:27:08.29
8	17	2	0:44:39.598 +41:25:40.59	0:44:40.648 +41:25:46.57
8	18	1	0:44:25.580 +41:26:40.59	0:44:24.938 +41:26:37.95
9	1	1	0:44:40.951 +41:37:06.63	No cluster
9	1	2	0:44:49.741 +41:39:14.20	0:44:50.573 +41:39:17.46
9	2	1	0:44:30.586 +41:37:44.86	0:44:31.445 +41:37:48.35
9	2	2	0:44:29.477 +41:39:00.50	0:44:30.138 +41:39:00.06
9	2	3	0:44:37.057 +41:37:26.24	0:44:36.770 +41:37:25.23
9	2	4	0:44:40.689 +41:37:09.91	No cluster
9	3	1	0:44:21.270 +41:39:28.88	0:44:22.259 +41:38:54.99
9	3	2	0:44:24.964 +41:38:30.43	0:44:26.525 +41:38:57.35
9	4	1	0:44:23.557 +41:40:47.91	0:44:24.030 +41:40:14.78
9	4	2	0:44:21.473 +41:40:04.78	0:44:24.030 +41:40:14.78
9	4	3	0:44:17.026 +41:38:44.81	0:44:15.096 +41:38:51.16
9	4	4	0:44:12.072 +41:39:48.34	0:44:10.854 +41:40:04.12
9	5	2	0:44:09.472 +41:39:58.67	0:44:04.131 +41:40:13.71
9	5	3	0:44:08.695 +41:39:33.04	0:44:06.992 +41:39:18.48
9	5	4	0:44:07.494 +41:39:49.27	0:44:06.992 +41:39:18.48
9	6	1	0:43:56.743 +41:42:01.33	0:44:00.767 +41:42:30.15
9	9	1	0:44:18.680 +41:35:31.37	0:44:20.531 +41:35:02.39
9	10	1	0:44:17.036 +41:38:44.71	0:44:15.102 +41:38:51.23
9	10	2	0:44:12.249 +41:38:41.10	0:44:13.819 +41:38:21.26
9	10	3	0:44:03.479 +41:38:31.08	0:44:03.512 +41:38:28.30
9	11	4	0:43:56.443 +41:38:08.56	0:43:56.543 +41:38:03.49
9	12	1	0:45:49.699 +41:38:07.60	0:43:51.977 +41:37:54.28
9	13	1	0:44:34.597 +41:33:29.29	0:44:31.863 +41:34:13.79
9	14	1	0:44:26.230 +41:33:14.43	0:44:23.068 +41:33:06.35
9	15	4	0:44:22.319 +41:35:51.23	0:44:23.321 +41:35:04.11
9	17	2	0:44:03.942 +41:36:52.25	0:44:02.858 +41:37:37.87
9	17	3	0:43:59.443 +41:38:08.56	0:43:56.552 +41:38:03.78
9	18	1	0:43:49.699 +41:38:07.60	0:43:51.980 +41:37:54.25
10	2	1	0:45:34.378 +41:33:39.37	0:45:35.953 +41:33:46.41
10	3	1	0:45:21.161 +41:33:27.23	0:45:23.033 +41:33:09.86
10	3	2	0:45:26.188 +41:34:46.91	0:45:28.513 +41:35:01.42
10	3	3	0:45:28.009 +41:34:33.28	0:45:29.071 +41:34:11.83
10	4	1	0:45:23.388 +41:35:57.87	0:45:23.385 +41:35:57.91
10	4	2	0:45:09.456 +41:34:30.17	No cluster
10	5	2	0:45:03.261 +41:35:52.07	0:45:02.914 +41:35:46.46
10	5	3	0:45:00.203 +41:36:43.54	0:45:02.563 +41:36:45.28
10	6	1	0:44:58.858 +41:36:51.71	0:44:59.857 +41:36:03.35
10	6	2	0:44:54.097 +41:35:08.28	0:44:54.003 +41:35:11.54
10	8	1	0:45:27.078 +41:30:13.08	0:45:26.066 +41:30:06.83
10	9	1	0:45:16.078 +41:33:04.44	0:45:17.332 +41:33:21.05
10	9	2	0:45:21.141 +41:33:27.33	0:45:23.099 +41:33:09.99
10	9	3	0:45:26.944 +41:32:09.72	No cluster
10	10	1	0:45:09.528 +41:33:37.79	0:45:10.853 +41:33:13.95
10	11	1	0:44:53.982 +41:34:05.78	No cluster

Table A.1 (cont'd)

Brick	Field	PN	PN Coordinates ^a	Cluster Coordinates ^b
10	12	2	0:44:35.951 +41:34:05.65	0:44:52.425 +41:34:04.4
10	17	2	0:44:50.290 +41:31:50.30	0:44:52.293 +41:32:01.93
10	18	2	0:43:49.709 +41:38:07.64	0:43:51.980 +41:37:54.25
11	1	1	0:45:02.016 +41:40:38.06	0:45:03.353 +41:40:05.11
11	1	2	0:45:10.309 +41:42:26.38	0:45:09.955 +41:42:23.37
11	2	1	0:44:53.817 +41:42:22.44	0:44:59.139 +41:42:25.57
11	3	1	0:44:44.186 +41:44:04.97	0:44:42.114 +41:43:54.61
11	3	2	0:44:44.599 +41:44:12.52	0:44:42.114 +41:43:54.61
11	4	1	0:44:31.791 +41:44:11.98	0:44:27.999 +41:44:10.48
11	5	1	0:44:20.106 +41:42:02.81	0:44:22.798 +41:41:39.12
11	5	2	0:44:16.331 +41:42:22.30	0:44:15.964 +41:42:11.77
11	6	1	0:44:13.407 +41:43:12.23	0:44:15.964 +41:42:11.77
11	6	2	0:44:12.496 +41:44:20.20	0:44:15.279 +41:43:55.27
11	6	3	0:44:08.580 +41:43:43.06	No cluster
11	6	4	0:44:09.578 +41:42:34.99	No cluster
11	7	1	0:45:00.389 +41:39:15.26	0:45:01.553 +41:39:04.41
11	11	2	0:44:16.326 +41:42:22.37	0:44:15.966 +41:42:11.93
11	14	1	0:44:40.943 +41:37:06.75	No cluster
11	16	4	0:44:17.043 +41:38:44.74	No cluster
12	1	1	0:46:00.621 +41:39:25.54	No cluster
12	1	2	0:46:05.013 +41:39:36.49	0:46:06.935 +41:39:49.43
12	2	1	0:45:53.698 +41:39:55.28	0:45:49.686 +41:39:26.39
12	4	1	0:45:26.698 +41:40:48.12	0:45:24.682 +41:40:50.51
12	4	2	0:45:27.004 +41:41:17.80	0:45:27.972 +41:42:03.68
12	5	1	0:45:24.378 +41:43:35.13	0:45:24.441 +41:43:28.56
12	5	2	0:45:18.453 +41:42:15.61	0:45:19.365 +41:42:27.61
12	6	1	0:45:14.930 +41:43:46.55	0:45:16.094 +41:43:21.99
12	6	2	0:45:13.757 +41:43:16.39	0:45:16.094 +41:43:21.99
12	7	3	0:45:53.769 +41:35:33.40	No cluster
12	8	1	0:45:46.868 +41:36:57.66	0:45:43.823 +41:37:45.20
12	8	2	0:45:49.170 +41:36:44.52	0:45:43.823 +41:37:45.20
12	11	1	0:45:14.476 +41:39:03.09	0:45:14.044 +41:38:21.51
12	13	1	0:45:47.378 +41:35:12.33	0:45:46.309 +41:35:27.92
12	13	2	0:45:51.016 +41:35:18.51	No cluster
12	15	3	0:45:28.883 +41:36:14.20	0:45:31.394 +41:36:14.31
12	16	1	0:45:26.004 +41:36:31.68	0:45:23.144 +41:36:28.14
12	16	2	0:45:23.623 +41:35:50.80	0:45:23.385 +41:35:57.91
12	17	1	0:45:12.484 +41:39:19.42	0:45:10.992 +41:38:56.41
12	17	2	0:45:16.632 +41:39:19.82	0:45:16.628 +41:39:19.86
13	1	1	0:45:11.691 +41:47:40.20	0:45:09.867 +41:47:21.35
13	1	2	0:45:12.514 +41:47:44.29	0:45:15.136 +41:47:31.96
13	1	3	0:45:10.469 +41:49:26.03	0:45:11.296 +41:49:20.36
13	3	3	0:44:49.471 +41:47:16.41	0:44:48.894 +41:47:59.06
13	3	4	0:44:48.528 +41:48:17.47	0:44:48.894 +41:47:59.06
13	4	1	0:44:37.446 +41:50:42.95	0:44:37.064 +41:50:43.59
13	4	2	0:44:38.546 +41:50:19.15	0:44:37.064 +41:50:43.59
13	4	3	0:44:36.777 +41:49:53.58	0:44:37.431 +41:49:33.79
13	7	1	0:44:57.397 +41:45:57.65	No cluster

Table A.1 (cont'd)

Brick	Field	PN	PN Coordinates ^a	Cluster Coordinates ^b
13	7	2	0:45:01.622 +41:45:46.95	0:45:02.960 +41:45:56.79
13	7	3	0:45:04.020 +41:46:07.06	0:45:04.072 +41:46:20.78
13	8	1	0:44:55.999 +41:45:45.90	0:44:55.589 +41:45:24.97
13	8	2	0:44:57.403 +41:45:57.70	0:45:00.064 +41:45:52.03
13	9	1	0:44:44.590 +41:47:05.30	No cluster
13	10	2	0:44:32.464 +41:46:37.75	0:44:32.598 +41:46:38.07
13	13	2	0:45:14.924 +41:43:46.50	0:45:16.392 +41:43:32.07
13	14	2	0:44:53.472 +41:43:04.58	0:44:59.139 +41:42:25.57
13	15	1	0:44:38.273 +41:43:53.35	0:44:40.420 +41:43:42.13
13	16	2	0:44:27.647 +41:44:29.42	0:44:27.999 +41:44:10.48
13	17	1	0:44:19.335 +41:46:08.60	No cluster
13	18	2	0:44:06.220 +41:45:59.46	0:44:06.332 +41:45:51.78
13	18	3	0:45:05.101 +41:45:14.67	0:44:02.468 +41:45:26.21
14	2	1	0:46:00.306 +41:45:46.79	0:46:00.018 +41:46:05.16
14	3	1	0:45:45.830 +41:47:05.76	0:45:45.559 +41:5:52.29
14	5	1	0:45:36.835 +41:47:20.49	0:45:40.445 +41:47:08.94
14	5	2	0:45:29.145 +41:48:21.80	0:45:29.271 +41:48:08.65
14	5	3	0:45:24.819 +41:47:31.07	0:45:22.274 +41:47:57.11
14	6	1	0:45:21.852 +41:46:50.23	0:45:19.185 +41:46:54.90
14	6	3	0:45:11.691 +41:47:40.02	No cluster
14	7	1	0:46:17.333 +41:43:28.61	No cluster
14	8	1	0:45:55.957 +41:43:15.44	No cluster
14	9	1	0:45:42.330 +41:44:29.44	0:45:39.854 +41:44:41.52
14	10	1	0:45:33.003 +41:45:24.68	0:45:35.585 +41:45:18.28
14	10	2	0:45:33.515 +41:44:53.33	0:45:35.625 +41:44:27.53
14	11	1	0:45:21.589 +41:44:36.88	0:45:20.484 +41:44:37.39
14	13	1	0:46:15.868 +41:42:01.28	0:46:15.204 +41:42:04.24
14	14	1	0:45:55.991 +41:43:15.97	No cluster
14	15	1	0:45:41.580 +41:49:43.65	No cluster
14	16	1	0:44:52.765 +41:49:43.65	0:44:52.563 +41:49:41.93
14	16	2	0:44:43.247 +41:50:49.45	0:44:41.829 +41:51:22.65
14	17	1	0:45:24.426 +41:43:35.13	0:45:27.146 +41:43:44.71
14	17	2	0:45:23.700 +41:43:29.19	0:45:27.146 +41:43:44.71
14	17	3	0:45:21.613 +41:44:36.34	0:45:23.404 +41:44:29.74
14	17	4	0:45:29.449 +41:41:36.80	No cluster
14	17	5	0:45:27.100 +41:41:17.52	No cluster
15	1	1	0:45:27.673 +41:55:40.88	0:45:26.025 +41:55:51.40
15	1	2	0:45:29.080 +41:55:47.26	0:45:28.888 +41:55:57.73
15	3	1	0:44:56.939 +41:54:29.31	0:44:56.565 +41:54:26.29
15	7	1	0:45:21.078 +41:52:08.05	0:45:19.175 +41:52:01.89
15	7	2	0:45:24.312 +41:51:59.73	0:45:24.953 +41:51:41.73
15	9	1	0:44:54.732 +41:53:05.22	0:44:54.382 +41:53:05.94
15	9	2	0:44:53.628 +41:53:25.80	0:44:52.980 +41:53:40.36
15	11	2	0:44:38.201 +41:52:10.66	0:44:38.181 +41:52:16.68
15	12	1	0:44:23.384 +41:53:36.28	0:44:26.038 +41:53:12.25
15	13	1	0:45:17.021 +41:49:53.60	0:45:13.763 +41:50:07.65
15	14	1	0:45:10.649 +41:49:26.03	0:45:11.307 +41:49:20.27
15	17	1	0:44:38.581 +41:53:02.75	0:44:38.350 +41:52:54.77

Table A.1 (cont'd)

Brick	Field	PN	PN Coordinates ^a	Cluster Coordinates ^b
15	17	4	0:44:38.549 +41:50:19.15	0:44:37.068 +41:50:43.58
16	2	1	0:46:18.347 +41:52:22.80	0:46:20.977 +41:52:28.40
16	3	1	0:46:07.070 +41:52:04.16	0:46:08.068 +41:52:12.99
16	4	1	0:45:59.722 +41:54:23.58	0:45:57.226 +41:53:31.02
16	4	2	0:45:53.836 +41:53:32.52	0:45:52.341 +41:53:46.10
16	4	3	0:45:49.648 +41:54:02.02	0:45:52.341 +41:53:46.10
16	5	2	0:45:44.648 +41:52:41.19	0:45:45.750 +41:52:10.01
16	5	3	0:45:42.685 +41:52:07.57	0:45:42.749 +41:51:50.99
16	7	1	0:46:19.117 +41:49:42.90	0:46:17.665 +41:49:45.27
16	8	1	0:46:08.135 +41:50:59.81	0:46:06.369 +41:50:37.20
16	8	2	0:46:13.649 +41:49:29.93	0:46:13.354 +41:49:21.61
16	9	1	0:46:01.923 +41:49:47.20	0:46:02.006 +41:50:04.60
16	11	1	0:45:40.817 +41:51:15.88	0:45:40.469 +41:51:17.67
16	11	2	0:45:37.821 +41:51:17.19	0:45:37.229 +41:51:09.23
16	13	1	0:46:23.296 +41:47:09.95	No cluster
16	13	2	0:46:29.249 +41:47:29.32	No cluster
16	14	1	0:46:07.310 +41:48:08.98	0:46:06.466 +41:48:22.30
16	16	1	0:45:45.881 +41:49:43.69	0:45:44.528 +41:49:21.61
17	1	2	0:45:46.212 +41:59:41.92	0:45:45.834 +41:59:21.77
17	2	1	0:45:38.440 +42:00:24.10	0:45:36.932 +42:00:06.93
17	3	1	0:45:23.043 +42:00:38.70	No cluster
17	4	1	0:45:22.673 +42:02:53.16	No cluster
17	4	2	0:45:17.721 +42:02:27.03	0:45:18.522 +42:01:51.20
17	6	1	0:44:55.868 +42:03:40.66	0:44:54.869 +42:03:31.69
17	6	2	0:44:55.020 +42:02:44.01	0:44:53.378 +42:02:33.38
17	6	3	0:44:56.511 +42:02:14.48	0:44:53.378 +42:02:33.38
17	7	1	0:45:42.940 +41:58:20.11	0:45:42.111 +41:58:08.48
17	8	1	0:45:43.834 +41:59:33.47	0:45:45.830 +41:59:21.76
17	11	1	0:45:03.545 +41:59:49.70	0:45:02.457 +41:59:33.90
17	11	2	0:45:03.000 +41:59:22.73	0:45:02.457 +41:59:33.90
17	11	3	0:45:03.406 +41:58:16.84	0:45:05.176 +41:57:54.61
17	12	1	0:44:54.749 +42:00:37.69	0:44:46.921 +42:00:11.15
17	13	2	0:45:54.949 +41:55:58.21	0:45:55.261 +41:56:06.27
17	14	2	0:45:46.555 +41:56:08.57	0:45:48.986 +41:55:54.28
17	15	1	0:45:17.959 +41:56:59.02	0:45:21.047 +41:56:41.86
18	2	1	0:46:43.911 +41:58:10.01	0:46:39.707 +41:58:48.11
18	9	1	0:46:26.216 +41:55:39.10	No cluster
18	9	2	0:46:34.727 +41:56:03.32	0:46:38.404 +41:55:53.23
18	11	1	0:46:09.285 +41:55:43.98	No cluster
18	13	1	0:46:44.647 +41:53:20.53	0:46:41.392 +41:53:53.91
18	16	1	0:49:09.285 +41:55:43.98	0:46:10.014 +41:54:57.72
18	17	1	0:46:04.873 +41:56:37.84	0:46:08.511 +41:57:19.35
18	18	2	0:45:46.561 +41:56:08.62	0:45:45.904 +41:56:01.11
19	1	1	0:46:16.002 +42:05:35.64	0:46:16.664 +42:05:11.46
19	2	1	0:46:06.168 +42:07:00.24	0:46:07.082 +42:07:16.99
19	2	2	0:46:07.364 +42:06:36.92	0:46:06.179 +42:06:05.10
19	2	3	0:46:16.002 +42:05:36.64	0:46:16.666 +42:05:11.18
19	3	1	0:45:57.271 +42:07:45.84	0:45:53.945 +42:07:28.79

Table A.1 (cont'd)

Brick	Field	PN	PN Coordinates ^a	Cluster Coordinates ^b
19	3	2	0:46:02.119 +42:07:38.40	0:46:06.186 +42:06:05.11
19	4	1	0:45:53.333 +42:08:49.34	0:45:49.726 +42:08:22.15
19	5	1	0:45:43.528 +42:02:24.15	0:45:45.512 +42:08:50.49
19	6	1	0:45:31.479 +42:08:36.46	0:45:36.945 +42:08:01.91
19	6	2	0:45:26.671 +42:08:33.03	No cluster
19	7	1	0:46:18.507 +42:03:08.00	0:46:22.348 +42:03:15.46
19	9	1	0:45:52.174 +42:04:05.18	0:45:49.924 +42:04:21.62
19	10	1	0:45:46.986 +42:04:43.13	0:45:49.924 +42:04:21.62
19	10	2	0:45:46.029 +42:03:33.09	0:45:44.543 +42:03:23.49
19	12	1	0:45:29.466 +42:04:21.78	No cluster
19	12	2	0:45:29.236 +42:04:44.47	No cluster
19	12	3	0:45:27.368 +42:04:42.71	No cluster
19	12	4	0:45:26.009 +42:05:24.11	0:45:23.658 +42:06:25.71
19	16	1	0:45:38.482 +42:02:55.81	0:45:38.842 +42:03:22.39
19	17	1	0:45:27.916 +42:02:58.20	0:45:28.384 +42:03:10.53
19	18	1	0:45:22.678 +42:02:53.16	0:45:23.122 +42:02:53.17
20	1	1	0:47:34.193 +42:04:07.63	0:47:30.795 +42:05:03.01
20	4	1	0:46:56.843 +42:05:59.87	0:46:57.748 +42:05:55.58
20	12	1	0:46:32.448 +42:03:41.68	0:46:31.714 +42:04:34.65
21	2	1	0:46:25.593 +42:12:49.83	0:46:30.307 +42:12:38.26
21	9	1	0:46:15.774 +42:09:19.62	0:46:12.796 +42:09:06.89
21	13	1	0:46:27.446 +42:08:29.97	0:46:26.924 +42:08:15.09
21	13	2	0:46:42.998 +42:07:54.83	No cluster
21	15	1	0:46:15.785 +42:09:19.71	0:46:12.803 +42:09:06.89
21	16	2	0:45:57.280 +42:07:45.91	No cluster
21	17	2	0:45:43.548 +42:09:24.15	0:45:45.501 +42:08:50.41
22	1	1	0:47:38.259 +42:08:54.17	No cluster
22	2	1	0:47:32.891 +42:11:36.46	No cluster
22	7	2	0:47:38.272 +42:08:54.28	No cluster
22	8	1	0:47:34.597 +42:08:23.49	0:47:28.786 +42:09:14.41
22	11	1	0:46:54.190 +42:08:15.25	No cluster
22	12	1	0:46:42.984 +42:08:34.79	0:46:40.532 +42:08:58.62
22	16	1	0:47:06.377 +42:07:15.38	0:47:08.220 +42:07:39.66
22	17	2	0:46:59.517 +42:07:42.07	No cluster
22	17	3	0:46:54.179 +42:08:15.16	No cluster
22	18	1	0:46:42.971 +42:07:54.98	0:46:38.493 +42:07:51.32
23	3	1	0:47:00.679 +42:18:50.48	0:46:58.786 +42:17:45.42
23	3	2	0:47:03.857 +42:19:35.44	No cluster
23	4	1	0:46:47.398 +42:18:36.64	0:46:45.216 +42:18:45.39
23	4	2	0:46:44.271 +42:18:09.33	0:46:45.216 +42:18:45.39
23	10	2	0:46:42.975 +42:15:16.72	0:46:41.956 +42:15:46.08
23	10	3	0:46:35.583 +42:17:10.35	0:46:35.603 +42:17:09.38
23	12	1	0:46:26.363 +42:16:10.85	0:46:25.263 +42:15:57.45
23	12	2	0:46:21.340 +42:16:59.65	0:46:23.403 +42:15:42.13
23	16	1	0:46:47.109 +42:12:18.42	0:46:50.191 +42:14:52.04

^aRA & Dec (J2000)^bCoordinates of nearest star cluster. RA & Dec (J2000)

Table A.2. PN Candidate Descriptions

Brick	Field	PN	Kind, Color ^a	Distance ^b	Explanation
1	1	1	OC,Red	25.7	
1	1	2	OC,Red	27.3	
1	1	3	GC	29.1	
1	2	1	GC	35.5	
1	3	1	GC	17.5	
1	7	1		23.4	
1	7	2	GC	20.3	
1	8	1		28.3	
1	9	1	GC	16.9	
1	12	1	OC, White	59.8	
1	13	2		on edge	
1	14	1		26 to edge	
1	14	2		23.8 to edge	
1	14	3	GC	25	
1	14	4	OC, White	42.6	
1	14	5	GC	43.6	
1	15	1		25.2	
1	15	2	GC	108.7	
1	15	4	GC	64.2	
1	18	2		51.1 to edge	
1	18	3		45.8 to edge	
1	18	4		16.4 to edge	
1	18	5	GC	37.1	
1	18	6		18.4 to edge	
1	18	7	GC	4.3	
2	5	1		13.6	
2	5	2		25.9	
2	5	3		70.9	
2	6	1		34.4	
2	6	2		14.96	
2	8	1		25.8	
2	8	2		37.9	
2	9	1	OC	0.63	PN was not identifiable
2	9	3			
2	9	4	OC, red	4.6	Exceptionally red
2	9	5	GC	32.2	Globular cluster
2	10	2		1.3	PN was not identifiable
2	10	3	OC, red	23.2	Very red
2	12	1			
2	15	1	OC	9	Open cluster
2	15	2	OC, red	32.1	Dim open cluster
2	17	1			
2	17	2	OC, Red	20.7	
2	17	3	OC, Red ?	13.8	Not sure if that is a cluster
2	17	4	OC, white, red	17.7	
3	1	1	OC, red	1.9	
3	1	2			
3	2	1	needs screen shot	36.3	

Table A.2 (cont'd)

Brick	Field	PN	Kind, Color ^a	Distance ^b	Explanation
3	2	2			
3	2	4			
3	3	1	?	40	
3	3	2	?	36.2	
3	3	3			
3	3	4			
3	3	5			
3	4	1	?	40.5	
3	4	2			
3	5	2			
3	5	3			
3	6	3	OC,White	36.3	
3	7	1	OC,White	6.4	
3	7	2	OC,White	9.5	
3	7	3	GC	42.4	
3	7	4	OC,White	29	
3	8	2	GC	65.4	
3	8	3	GC	64	
3	9	1		5.1 to edge	
3	9	2	GC	36.9	
3	9	3		59.9 to edge	
3	10	2	GC	24	Closest cluster
3	11	1	GC	71.9	
3	11	2	OC,White	69.4	Lots of associations around PN
3	11	3	OC	48.6	Closest cluster
3	11	4	OC	51.2	Closest cluster
3	12	1	OC,White	65.2	Cluster is in between the two images
3	12	2	OC,White	17.6	
3	12	3			
3	13	2	GC	34.5	
3	14	1	?	62.4	
3	15	1		24.8	
3	15	2	GC	35.5	
3	17	2			
4	1	1		61.4	Closest cluster
4	2	1	OC,White	4.7	
4	3	2	OC,White	4.3	
4	4	1		13.2 to edges	
4	4	2	OC, red	3	Not sure if its an actual cluster
4	4	3	OC, white, red	25	
4	4	4	OC,White	21.3	
4	5	1	OC,White	26.4	
4	5	2	OC,White	2.9	
4	6	1	GC	11.2	
4	6	2	GC	13.5	
4	6	3		1.8	Good one
4	7	1	GC	53.5	
4	8	1	OC,White	28.9	

Table A.2 (cont'd)

Brick	Field	PN	Kind, Color ^a	Distance ^b	Explanation
4	10	2	OC,White	24.8	
4	10	3	OC,White	10.8	
4	12	2	OC,White	42.3	
4	14	3	OC,White	48.7	
4	14	4		32.6	
4	15	1	OC,White	40.8	
4	15	2	OC, white, red	10.1	
4	15	3	OC,White	32.9	
4	17	1	OC,White	12	
4	18	2	GC	26	
4	18	3	GC	13.7	
5	1	1	OC,White	18.5	
5	1	2		16.3	
5	1	4		30 to edge	
5	2	3		18.4	
5	3	2	OC,White	65.6	
5	3	5	GC	54.5	
5	4	1	OC,White	12.4	
5	4	3	OC,White	31	Lots of foggy spots around PNe
5	4	5		31.1	
5	5	1	OC,White	41.1	
5	5	2	OC,White	44.9	
5	5	3	OC,White	52.9	
5	5	4		39.1	
5	5	5		57.8	
5	5	6		12.5	
5	5	7		15.3 to edge	
5	5	8	GC	13.8	
5	6	5		28.3	
5	6	6		8.7	
5	9	1		19.5 to edge	
5	9	2		42.1	
5	9	3		on edge	
5	11	1		15 to edge	
5	11	2		14.9 to edge	
5	11	3		13.7	
5	11	5	GC	45	
5	12	3		12.3	
5	12	4	OC, red	72.4	
5	12	5		31.6	
5	12	6		11.3	
5	13	1	GC	37.1	
5	13	4		20.8	
5	13	5		16	
5	13	6		on edge	
5	14	1		21.2	
5	14	2	OC,White	9.8	
5	14	3		27.5	

Table A.2 (cont'd)

Brick	Field	PN	Kind, Color ^a	Distance ^b	Explanation
5	14	5		37.1	
5	15	6		40.5	
5	17	1	GC	45	
5	17	2	GC	79.1	
5	17	5		51.3	
5	17	7		on edge	
5	18	2		38.1	
5	18	4		17.4	
5	18	5		12.3 to edge	
5	18	6		23.1 to edge	
6	1	1		25.3	
6	1	2	OC, White	16.9	
6	4	1	OC, red	20.4	Close to associations
6	4	2	OC, White	22.9	
6	4	4	OC, White	15.6	
6	5	1	OC, White	11.2	Not sure if it's an actual cluster
6	5	2	OC, red	4.8	
6	5	3	OC, red	24.4	
6	5	5	OC, White	22.5	
6	6	1	OC, White	29.7	
6	6	2	GC	29.9	
6	6	5	GC	44.3	
6	7	1		59.7	
6	9	1	OC, red	0.8	Not sure if it's an actual cluster
6	10	2		10	
6	11	3	OC, White	6.3	Lots of star clumps and associations
6	11	4	OC, White	23.6	
6	11	5	GC	31	
6	12	3	OC, White	10.5	
6	12	4	OC, White	11.2	
6	13	2		on edge	
6	13	3	OC, White	36.8	
6	13	4	OC, White	27.7	
6	16	1	OC, White	4.2	
6	17	1		23.5	
6	17	3	OC, White	42.4	
6	18	2	OC, White	11.3	
7	1	1	OC, White	16.4	
7	1	2		15.2	
7	1	3	OC, White	21.3	
7	2	1	OC, White	14	
7	2	2	Big group of cluster	16.6	Not sure if its an actual cluster
7	2	3		15.9	
7	2	4	OC, White	51.5	
7	2	5		22.5	
7	3	2		49.7	
7	3	4	OC, White	3.1	Surrounded by associated stars
7	4	2		35.8	

Table A.2 (cont'd)

Brick	Field	PN	Kind, Color ^a	Distance ^b	Explanation
7	4	3	OC,White	18.9	
7	5	2	OC,White and red	9.8	
7	5	4	OC,White	7.5	
7	5	5	OC,White	31.7	
7	5	7	OC,White	18.7	
7	5	8		on edge	
7	6	2	OC,White and red	18.7	
7	6	3		12.8	
7	6	4		on edge	
7	7	1		20.6	
7	7	2		60.3	
7	7	5	OC,White	39.6	
7	8	1	GC	19.5	
7	8	2	GC	31.9	
7	8	5		56.8	
7	10	1		59.7	
7	10	2	GC	32.2	Small GC
7	11	3	OC,White	6.2	
7	11	6	GC	26.9	
7	12	2	OC,White	12.8	Cluster is very dim and small
7	12	3	OC,White	24.8	
7	13	2		24.8 to the edge	Lots of star clumps and associations
7	13	3		65.4 to the edge	
7	14	1	OC,White	16.3	
7	14	2	OC,White	21.5	Not sure if it's an actual cluster
7	15	1	OC,White	28.5	
7	16	3	OC,White	51.3	
7	17	1		18.6 to the edge	
7	17	3	OC,White	51	
7	17	4	OC,White	27.8	
7	18	1	OC,White	33.2	
7	18	3		on the edge	
8	4	1	OC,White	29.9	
8	4	2	OC,White, red	1.7	Lots of associations around
8	5	1		5	
8	5	3		20.6	
8	6	1		15 to the edge	
8	6	2		15.2	Not sure if it's an actual cluster
8	7	1		11.9	
8	8	2	OC,White	19	
8	8	3	OC,White	59	
8	9	1	OC,White	26.6	
8	9	2		13	
8	11	2	OC,White	3	
8	12	1	OC,White	43.6	
8	12	3	OC,White	63.5	
8	13	1	GC	13.2	
8	13	2	OC,White	11.8	

Table A.2 (cont'd)

Brick	Field	PN	Kind, Color ^a	Distance ^b	Explanation
8	14	2		10.1 to edge	
8	17	1	OC,White	3	
8	17	2	OCWhite	12.4	Not sure if it's an actual cluster
8	18	1	OC,White	8.3	Not sure if it's an actual cluster
9	1	1		21.3 to edge	
9	1	2	OC,Red	9.3	
9	2	1	OC,White and red	10.4	
9	2	2	OC,White	7.3	Dim, not sure if it's an actual cluster
9	2	3	OC,White	2.6	
9	2	4		26.4 to edge	
9	3	1	OC,White	36.1	
9	3	2	OC,White	32.2	Surrounded by 3 open clusters at the same distance
9	4	1	OC,White	34.9	
9	4	2	OC,White	29.6	
9	4	3	OC,White	22.9	PN color is white. Not sure if an actual PN
9	4	4	OC,White	21.2	Not sure if its an actual cluster
9	5	2	OC,White	15	Star surrounded by lots of star clumps
9	5	3	OC,White	24.7	Star surrounded by lots of star clumps
9	5	4	OC,Not sure	31.3	
9	6	1	OC,Red,Dim	53.9	
9	9	1	OC,White	36	
9	10	1		22.8	PN color is white. Not sure if an actual PNE
9	10	2	OC,White and red	26.8	
9	10	3	OC,White	3.6	Hard to identify the PNE
9	11	4	OC,White	6	
9	12	1	OC,White	29.2	
9	13	1	OC,White	53.8	
9	14	1	GC	37.6	
9	15	4	OC,White	48.6	
9	17	2	OC,White	47.1	
9	17	3	OC,White	5.6	
9	18	1	OC,White	29.2	
10	2	1	OC,White	17.8	
10	3	1	OC,White	28.3	
10	3	2	OC,White	30.3	
10	3	3	OC, white	25.1	
10	4	1	OC,White	7.9	
10	4	2		10.1 to the edge	
10	5	2	OC,White	6.6	Lots of star clumps and associations
10	5	3	OC,White	27.3	
10	6	1	OC,White	49.5	
10	6	2	OC,White	3	
10	8	1	OC,Red, Dim	12.3	Small clump most likely
10	9	1	OC,White	21	
10	9	2	OC,White	28.3	Small clump most likely
10	9	3		47.9 to edge	
10	10	1	OC,White	27.8	
10	11	1		on edge	Lots of star clumps

Table A.2 (cont'd)

Brick	Field	PN	Kind, Color ^a	Distance ^b	Explanation
10	12	2	OC,White	17.2	
10	17	2	OC,White	24.7	Lots of stars around
10	18	2	OC,White	29.3	
11	1	1	OC, red	36.6	
11	1	2	OC,White	4.4	
11	2	1	OC,White	60.2	
11	3	1	GC	25.2	Not sure if PN. Color was white
11	3	2	GC	32.8	
11	4	1	GC	42.1	
11	5	1	OC, red	38.1	
11	5	2	OC,White	11.3	
11	6	1	OC,White	66.8	
11	6	2	OC,White	40	Not sure if it's an actual cluster
11	6	3		72.8 to edge	PNE between two images so not visible in this field
11	6	4		71.5 to edge	
11	7	1	OC,White	16.6	Cluster not very visible, in between the gap
11	11	2	OC,White	11.1	
11	14	1		17.2 to edge	
11	16	4		on edge	
12	1	1		40.2 to edge	
12	1	2	OC,White	25.6	
12	2	1	OC,White	55	
12	4	1	OC,White	23.1	
12	4	2	OC,White	47.1	
12	5	1	OC,White	6.5	
12	5	2	OC,White	15.7	
12	6	1	OC,White	28	3 clusters close
12	6	2	OC,White	27.1	Can't identify the PN
12	7	3		40.9 to edge	
12	8	1	OC,White	58.6	
12	8	2	OC,White	85.7	
12	11	1	?	41.8	Lots of star clumps and associations
12	13	1	OC,Red	19.2	
12	13	2		44.6 to edge	
12	15	3	OC,White	27.6	
12	16	1	OC,White	32.7	
12	16	2	OC,White	8	Not sure if it's an actual cluster
12	17	1	OC,White	28.9	
12	17	2	OC,White	29.8	
13	1	1	OC,White	27.4	
13	1	2	OC,White	32.5	
13	1	3	OC,White	9.2	Lots of stars around
13	3	3	OC,White	32.5	
13	3	4	OC,White	19.1	
13	4	1	OC,White	5.7	Cluster is wide
13	4	2	OC,White	28.8	
13	4	3	OC,White	20.6	
13	7	1		on edge	

Table A.2 (cont'd)

Brick	Field	PN	Kind, Color ^a	Distance ^b	Explanation
13	7	2	OC,White	17.9	
13	7	3	OC,White	13.7	
13	8	1	OC,White	21.6	
13	8	2	OC,Red	30.4	
13	9	1		55.1 to edge	
13	10	2	OC,White	1.8	PN very close to outline of the cluster
13	13	2	OC,White	22.3	
13	14	2	OC,White	74.9	
13	15	1	GC	26.8	
13	16	2	GC	18.9	
13	17	1		21.1 to edge	
13	18	2	OC,White	7.4	
13	18	3	OC,White	31.3	
14	2	1	OC,White	18.7	
14	3	1	OC,White	73.5	Not closer than edge
14	5	1	OC,White	42.2	
14	5	2	OC,White	13.3	
14	5	3	OC,White	38.4	Lots of clumps and associations
14	6	1	OC,White	29.7	
14	6	3		17.2 to edge	
14	7	1		29.9 to edge	
14	8	1		72.2 to edge	
14	9	1	OC,White	50	
14	10	1	OC,White	30	
14	10	2	OC,White	35.2	
14	11	1	OC,White	12.4	
14	13	1	OC,White	7.8	
14	14	1		29.4 to edge	
14	15	1		24.1 to edge	
14	16	1	OC,Red	3.1	Not sure if it's an actual cluster
14	16	2	OC,White	37.1	
14	17	1	OC,White	32.3	
14	17	2	OC,White	41.6	Can't identify the PN
14	17	3	OC,White	21.5	Can't identify the PN, closest cluster
14	17	4		on edge	
14	17	5		on edge	
15	1	1	OC,White	21.4	
15	1	2	OC,Red	10.5	
15	3	1	OC,White	5.3	
15	7	1	OC,White	22	
15	7	2	OC,White	19.8	
15	9	1	OC,White	3.6	
15	9	2	OC,White	16.9	Not sure if PN, lots of star associations
15	11	2	OC,White	5.7	Lots of star clumps and associations
15	12	1	OC,White	38.4	
15	13	1	OC,White	39.4	
15	14	1	OC,White	9.4	
15	17	1	OC,White	8	Lots of star clumps and associations

Table A.2 (cont'd)

Brick	Field	PN	Kind, Color ^a	Distance ^b	Explanation
15	17	4	OC, White	28.8	
16	2	1	OC, White	30.3	
16	3	1	OC, White	14.3	
16	4	1	OC, White	60.1	
16	4	2	OC, White	21.5	
16	4	3	OC, White	34.4	
16	5	2	OC, White	34.6	
16	5	3	OC, White	16.3	
16	7	1	OC, White	16.9	
16	8	1	OC, White	29.8	
16	8	2	OC, White	8.9	
16	9	1	OC, White	18	
16	11	1	OC, White	3.8	
16	11	2	OC, White	10.4	
16	13	1		53.8 to edge	
16	13	2		28.8 to edge	
16	14	1	OC, White	16.4	
16	16	1	OC, White	27	
17	1	2	OC W or Small GC?	20.6	
17	2	1	OC, White	24.1	
17	3	1		25.1 to edge	
17	4	1		21 to edge	
17	4	2	OC, White	36.6	
17	6	1	OC, White	14.4	
17	6	2	OC, White	21	
17	6	3	OC, White	38.6	
17	7	1	OC, White	14.5	
17	8	1	OC, White	25.2	
17	11	1	OC, White	19.3	
17	11	2	OC, White	12.6	
17	11	3	OC, White	30	
17	12	1	OC, White	99	
17	13	2	OC, White	9	
17	14	2	OC, White	30.7	
17	15	1	OC, White	35.7	
18	2	1	OC, White	60.4	More like a clump of stars
18	9	1		14.2 to edge	
18	9	2	OC, White	42.6	Mostly associations
18	11	1		8.8 to edge	
18	13	1	OC, White and red	49.7	
18	16	1	OC, White	47.4	
18	17	1	OC, White	58.3	
18	18	2	OC, White	10.8	
19	1	1	OC, White	25.6	
19	2	1	OC, Red	19.1	
19	2	2	GC	35.5	
19	2	3	OC, White	25.7	
19	3	1	OC, White	40.2	

Table A.2 (cont'd)

Brick	Field	PN	Kind, Color ^a	Distance ^b	Explanation
19	3	2	GC	103.7	
19	4	1	OC, White	49.1	Closest cluster
19	5	1	OC, White	40.1	Closest cluster
19	6	1	OC, White	70.6	
19	6	2		54.1 to edge	
19	7	1	OC, White	43.3	
19	9	1	OC, White	29.6	
19	10	1	OC, White	39	
19	10	2	OC, White	19.5	
19	12	1		21 to edge	
19	12	2		38.9 to edge	
19	12	3		51.6 to edge	
19	12	4	OC, White	66.5	
19	16	1	OC, White	26.9	
19	17	1	OC, White	13.7	
19	18	1	OC, White	4.8	Not sure if its an actual cluster
20	1	1	OC, White	66.9	
20	4	1	OC, White	10.9	
20	12	1	A	53.1	
21	2	1	OC, White	53.7	Lots of star clumps and associations
21	9	1	OC, White	35.7	
21	13	1	OC, White	15.3	
21	13	2		30.4 to edge	
21	15	1	OC, White	35.8	
21	16	2		on edge	
21	17	2	OC,Red	40.1	
22	1	1		15.3 to edge	
22	2	1		63.2 to edge	
22	7	2		67.1 to edge	
22	8	1	OC, White	82.8	
22	11	1		20.8 to edge	
22	12	1	OC, White	35.6	
22	16	1	OC, White	31.5	
22	17	2		77 to edge	
22	17	3		65.5 to edge	
22	18	1	A	50.8	
23	3	1	OC, White	68.4	
23	3	2		26.2 to edge	
23	4	1	OC, White	25.6	
23	4	2	OC, White	37.5	
23	10	2	OC, White	32.2	
23	10	3	OC,White	2	
23	12	1	OC,Red	17.5	
23	12	2	OC,White	77.6	
23	16	1	OC, White	44.1	

^aGC=Globular Cluster; OC=Open Cluster; A=Association

^bDistance from PN to cluster in arcseconds.

APPENDIX B

TABLE OF PN PARAMETERS

Table B.1. PN Candidate Photometry

ID	RA (deg)	Dec (deg)	Flux (counts)	Flux (ergs/sec/cm ² /Å)	Mag
1	11.75273312	42.31408254	2701.062	3.52939E-15	22.4393902
2	11.76590136	42.3267119	154.0861	2.01339E-16	25.50017931
3	11.69743366	42.31031517	1934.902	2.52827E-15	22.8363454
4	12.01472048	42.61062299	8929.688	1.16681E-14	21.09249726
6	11.79962649	42.51313863	10083.82	1.31762E-14	20.96052526
7	12.04062023	42.52369804	1245.911	1.62799E-15	23.23087042
8	11.8146682	42.4780812	949.2291	1.24033E-15	23.52616036
9	12.01595932	42.42759741	1902.684	2.48617E-15	22.7711713
10	11.97780714	42.43060953	642.6445	8.39722E-16	23.94966098
11	11.88160329	42.43850285	3706.929	4.84372E-15	22.0470523
12	11.75114581	42.45534483	2360.158	3.08394E-15	22.53723528
13	11.48475022	42.44268406	903.6006	1.1807E-15	23.57964669
14	11.40609606	42.40801697	2474.352	3.23315E-15	22.48593426
15	11.56047604	42.41662243	1228.471	1.6052E-15	23.2461757
16	11.50732923	42.40687848	742.2955	9.69933E-16	23.7931459
17	11.65084658	42.39258662	2192.206	2.86448E-15	22.61738456
18	11.7310853	42.40063483	15794.91	2.06387E-14	20.47329508
19	11.89535828	42.38261613	6940.926	9.06948E-15	21.36604443
20	11.96233123	42.34058348	1642.671	2.14642E-15	22.93071149
21	11.44562028	42.28765241	2292.907	2.99607E-15	22.635217
22	11.48326539	42.28265196	1428.453	1.86651E-15	23.1818054
23	12.12882424	42.30857125	3761.745	4.91535E-15	22.03111459
24	12.05480143	42.29355918	335.4771	4.38357E-16	24.65543077
25	12.10343043	42.28522513	1423.628	1.86021E-15	23.08609667
26	11.87835717	42.28312361	593.1384	7.75034E-16	24.8300285
27	11.69613261	42.25544487	4952.152	6.47081E-15	21.8648574
28	11.67906126	42.25453406	2614.041	3.41568E-15	22.563451
29	11.64805779	42.28653185	2148.886	2.80788E-15	22.6525177
30	11.68419541	42.3027544	1159.518	1.5151E-15	23.3081288
31	11.60948836	42.2697512	465.7956	6.0864E-16	24.1362982
32	11.58845929	42.2822326	2231.078	2.91528E-15	22.7430303
33	11.52960252	42.26603558	4540.694	5.93317E-15	21.9458454
34	11.35606309	42.23636624	871.5302	1.1388E-15	23.7009296
35	11.97312412	42.24948352	6150.14	8.03618E-15	21.49737546
36	12.04690483	42.23843274	984.2552	1.28609E-15	23.48681867
38	11.94468047	42.20424771	11586.66	1.51399E-14	20.80969231
39	11.99834985	42.19229735	720.02	9.40826E-16	23.82622657
40	12.0970278	42.20417198	556.369	7.26989E-16	24.10618066
41	11.88701104	42.19349827	11049.74	1.44383E-14	20.9864766
42	11.60656439	42.21397449	734.2498	9.5942E-16	24.3096456
44	11.36092852	42.14277185	1315.398	1.71879E-15	23.2297026
46	11.43160587	42.15690386	2239.812	2.92669E-15	22.6753738
47	11.47222245	42.14738897	4227.801	5.52433E-15	22.008572
48	11.56567177	42.15581618	2059.62	2.69124E-15	22.68512022
49	11.67883351	42.14322582	15478.03	2.02246E-14	20.5693291
50	11.72589787	42.13773865	1061.487	1.38701E-15	23.5939734
51	11.61397879	42.14162404	1604.328	2.09632E-15	23.1142176
52	11.89414068	42.13985509	424.3062	5.54427E-16	24.40038952

Table B.1 (cont'd)

ID	RA (deg)	Dec (deg)	Flux (counts)	Flux (ergs/sec/cm ² /Å)	Mag
53	11.90924499	42.14844723	365.8646	4.78063E-16	25.0414291
54	11.74796063	42.13022175	1505.387	1.96704E-15	23.1216541
55	11.77637838	42.12099003	12061.98	1.5761E-14	20.8565804
56	11.73677111	42.10008501	1910.851	2.49685E-15	23.0055888
57	11.52582888	42.11694523	5908.125	7.71995E-15	21.6517223
58	11.53093822	42.11058938	1614.668	2.10983E-15	22.990402
59	11.56630195	42.09331513	5393.457	7.04745E-15	21.7154777
60	11.67903852	42.13210071	343.1241	4.48349E-16	24.5202766
61	11.48832652	42.12942832	10388.96	1.35749E-14	21.0248551
62	11.50884248	42.12747247	1078.999	1.40989E-15	23.8020747
63	11.46712406	42.06816687	1341.694	1.75315E-15	23.1799656
64	11.3642072	42.0786028	1682.676	2.1987E-15	23.0517252
65	12.00992263	42.09061378	980.6037	1.28132E-15	23.49085415
66	11.98062262	42.06553086	2733.52	3.5718E-15	22.37778233
67	11.8921672	42.06897057	6990.315	9.13401E-15	21.4624111
68	11.63500219	42.06173294	3863.621	5.04846E-15	22.0375627
69	11.5771052	42.05227563	1852.86	2.42107E-15	22.7975438
70	11.46827239	42.03701338	3643.635	4.76102E-15	22.1147075
71	11.44166988	42.05943843	2983.066	3.89787E-15	22.3739253
87	11.41002747	42.00684174	1313.337	1.71609E-15	23.17364752
190	11.35812924	42.09021372	1125.307	1.4704E-15	23.4429281
192	11.36618271	42.04953159	1404.231	1.83486E-15	23.2266078
193	11.41034325	42.04895993	469.5594	6.13558E-16	24.2969052
194	11.37188817	42.07900211	388.6699	5.07862E-16	24.6101523
195	11.37245624	42.07285013	865.284	1.13064E-15	23.8552437
196	11.44582216	42.07892651	708.2537	9.25452E-16	23.9519913
43	11.34896987	42.21725035	574.3953	7.50543E-16	24.07156078
72	11.22818053	42.29405163	4546.716	5.94104E-15	21.8253434
73	11.32893034	42.21247598	2505.378	3.27369E-15	22.47240482
74	11.30969015	42.19919584	1469.934	1.92071E-15	23.05134338
75	11.21772059	42.19940458	5238.657	6.84518E-15	21.67153806
76	11.23107336	42.22953227	531.5787	6.94596E-16	24.15566904
77	11.23518139	42.24197727	1289.117	1.68445E-15	23.19385713
78	11.19987017	42.19849014	1881.553	2.45856E-15	22.78329683
79	11.21191726	42.08514754	2666.631	3.4844E-15	22.3097223
81	11.2228798	42.07360564	1783.704	2.33071E-15	22.7657104
82	11.31278032	42.09968139	3113.692	4.06856E-15	22.1839696
84	11.45443362	41.99402512	4158.409	5.43365E-15	21.9081618
85	11.42883998	41.97225085	7198.809	9.40644E-15	21.2549321
86	11.43252922	41.99262196	1059.997	1.38506E-15	23.2693747
88	11.34572922	42.01084868	1473.296	1.92511E-15	23.0066705
89	11.26399747	41.97140759	7987.621	1.04372E-14	21.1519006
93	11.32462648	41.94710851	6819.562	8.91089E-15	21.3055327
94	11.36529537	41.92800059	5915.333	7.72937E-15	21.4823229
95	11.37107274	41.92998098	6999.122	9.14552E-15	21.2904196
96	11.44403651	41.9359241	1702.401	2.22447E-15	22.9133792
97	11.52023561	41.94396091	5864.747	7.66327E-15	21.4745618
98	11.53876493	41.92906139	5264.381	6.87879E-15	21.565927

Table B.1 (cont'd)

ID	RA (deg)	Dec (deg)	Flux (counts)	Flux (ergs/sec/cm ² /Å)	Mag
99	11.60923987	41.92758777	3484.606	4.55322E-15	22.0223959
100	11.682819	41.96947878	909.0895	1.18788E-15	23.598384
101	11.78866333	41.93706514	5630.426	7.35709E-15	21.59323483
102	11.68606968	41.88913733	3057.875	3.99562E-15	22.1957347
103	11.47410666	41.892399	4583.286	5.98883E-15	21.7924262
104	11.47890478	41.93294378	2258.283	2.95082E-15	22.5305088
105	11.22343568	41.89046451	8884.618	1.16092E-14	20.9978651
106	11.23719851	41.90831412	2753.562	3.59799E-15	22.1786497
107	11.16067129	41.88410527	3906.173	5.10407E-15	22.137107
108	11.22791432	41.88496433	1110.717	1.45134E-15	23.343574
109	11.33774068	41.868934	1578.12	2.06208E-15	22.6804295
110	11.40753126	41.85494035	928.0219	1.21262E-15	23.2011918
111	11.4198727	41.85454644	3196.304	4.1765E-15	22.0122731
112	11.35112033	41.86677819	2179.335	2.84766E-15	22.5820848
113	11.42777064	41.86883359	2033.433	2.65702E-15	22.5650932
114	11.57629429	41.87296968	7244.813	9.46656E-15	21.2866738
115	11.45628594	41.90094045	6024.912	7.87255E-15	21.5197112
116	11.90022201	41.85961346	3085.828	4.03215E-15	22.24615868
117	11.92141431	41.83442665	3101.408	4.05251E-15	22.24069071
118	11.57966074	41.82863066	2131.049	2.78457E-15	22.6420001
119	11.55665087	41.82511	13387.87	1.74935E-14	20.6093651
120	11.44103305	41.8290582	9766.667	1.27618E-14	20.8683328
121	11.5077923	41.82986704	9549.011	1.24774E-14	20.949383
122	11.53030776	41.8025773	4388.406	5.73418E-15	21.7658426
124	11.66776443	41.76288801	1216.427	1.58946E-15	23.2401036
125	11.59691234	41.78620797	2295.479	2.99943E-15	22.5167932
126	11.62188734	41.79159857	566.3609	7.40045E-16	23.8645229
128	11.44069985	41.78499978	2087.689	2.72791E-15	22.6269182
129	11.40343431	41.78910144	3194.767	4.1745E-15	22.1666998
130	11.35344268	41.79215066	4880.793	6.37757E-15	21.647267
131	11.30201709	41.79592243	5564.958	7.27155E-15	21.5950066
132	11.29875728	41.79443895	8740.854	1.14214E-14	21.0618073
133	11.26664441	41.76876246	10009.29	1.30788E-14	20.9396192
134	11.18581164	41.78502944	2358.102	3.08125E-15	22.4969693
135	11.20629787	41.78806629	6909.955	9.02901E-15	21.2861611
136	11.21112361	41.7927656	4305.723	5.62614E-15	21.7828076
137	11.20199279	41.80500747	8244.74	1.07731E-14	21.0981723
138	11.21983474	41.82904276	4986.309	6.51544E-15	21.6755156
139	11.15300455	41.83147435	6917.468	9.03882E-15	21.3037711
140	11.13517525	41.77729428	6048.61	7.90352E-15	21.4803004
141	11.23917227	41.76618837	903.4495	1.18051E-15	23.4963703
142	11.32105658	41.83167282	4731.315	6.18225E-15	21.7214608
143	11.24938998	42.12917266	4160.032	5.43578E-15	21.92184629
144	11.14686229	42.25878256	1197.35	1.56454E-15	23.27403517
145	11.72987912	41.78947896	1488.859	1.94544E-15	23.03745404
146	11.37128404	41.80616101	1627.326	2.12637E-15	22.8492132
147	11.25669411	41.7631134	1775.439	2.31991E-15	22.8612307
148	11.16029741	41.83885654	5561.383	7.26687E-15	21.5165263

Table B.1 (cont'd)

ID	RA (deg)	Dec (deg)	Flux (counts)	Flux (ergs/sec/cm ² /Å)	Mag
150	11.64465082	41.93444267	2572.621	3.36156E-15	22.0480426
151	11.77038159	41.94418091	361.9038	4.72888E-16	24.57310511
152	11.77171117	41.9501037	423.5236	5.53404E-16	24.40239393
153	11.53366111	41.85011693	2439.351	3.18742E-15	22.4433748
154	11.52924063	41.8680897	865.7505	1.13125E-15	23.8128312
155	11.49873077	41.9068031	882.8289	1.15356E-15	23.368743
156	11.43604116	41.87815516	3228.73	4.21887E-15	22.0055734
157	11.26456675	41.99720536	605.5626	7.91268E-16	24.0490943
158	11.2625293	41.9897899	1182.396	1.545E-15	23.3135661
160	11.29433554	41.82399714	1645.845	2.15057E-15	22.8251437
161	11.28775554	42.09093509	2398.549	3.1341E-15	22.4626358
162	11.13292655	42.07870795	1222.594	1.59752E-15	23.2130939
163	11.12481976	42.08103172	1374.725	1.79631E-15	23.160291
179	11.16777229	42.06974127	891.72	1.16518E-15	23.5481091
180	11.18233943	42.07614603	1803.805	2.35697E-15	22.829114
181	11.1990936	42.07689778	1713.987	2.23961E-15	22.8028451
185	11.23186314	42.073401	959.9746	1.25437E-15	23.2977679
186	11.23282512	42.06144637	638.8785	8.34801E-16	23.7221537
187	11.23897497	42.07303648	1571.571	2.05352E-15	23.1127216
188	11.23532273	42.03824118	824.7709	1.0777E-15	23.4652164
189	11.27018562	42.06847777	835.6735	1.09195E-15	23.66449639
191	11.3445995	42.04808514	1175.367	1.53581E-15	23.29415424
198	11.44251319	41.9951641	1611.773	2.10605E-15	22.8949438
306	11.15915168	41.86985572	1904.719	2.48883E-15	22.77001068
307	11.18000075	41.84705644	228.5209	2.98601E-16	25.07227315
322	11.34081007	41.78073703	576.2853	7.53013E-16	23.5452991
340	11.23318869	41.76289421	789.8823	1.03211E-15	24.0392983
80	11.22055967	42.05987318	1111.252	1.45204E-15	23.35505658
83	11.19719014	42.04991776	1333.909	1.74297E-15	23.15677246
87	11.41003211	42.00684126	1518.522	1.9842E-15	23.01603525
90	11.22777704	42.01046836	242.9411	3.17443E-16	25.00583549
91	11.12705334	42.00986894	7661.762	1.00114E-14	21.25876633
92	11.10721806	41.99928125	5456.47	7.12979E-15	21.62730854
127	11.50104177	41.76310687	2231.91	2.91636E-15	22.59789627
159	11.323699	42.04085208	662.5135	8.65684E-16	23.91660114
164	11.12189807	42.06849662	1936.443	2.53029E-15	22.75207617
165	11.09805118	42.0898835	1538.909	2.01084E-15	23.00155562
166	11.10034487	42.09340668	1382.946	1.80705E-15	23.11757491
167	10.97560371	42.0443515	1629.393	2.12907E-15	22.93952335
168	11.04241292	42.05838459	2280.809	2.98026E-15	22.57436567
169	11.0835654	42.03295265	1457.037	1.90386E-15	23.06091152
170	11.0682487	42.05644166	1099.638	1.43686E-15	23.36646362
171	11.06319598	42.04696196	957.5295	1.25117E-15	23.51670756
172	11.06338302	42.05510033	886.0737	1.1578E-15	23.60091335
173	11.05817482	42.08112467	1208.779	1.57947E-15	23.2637207
175	11.07526625	42.07389256	933.4672	1.21973E-15	23.54434031
176	11.09569809	42.06150881	1437.805	1.87873E-15	23.075338
177	11.09243068	42.06707758	1244.547	1.62621E-15	23.23205971

Table B.1 (cont'd)

ID	RA (deg)	Dec (deg)	Flux (counts)	Flux (ergs/sec/cm ² /Å)	Mag
178	11.0491887	42.03542451	1143.785	1.49455E-15	23.32372698
182	11.13394013	42.05383769	1010.373	1.32022E-15	23.45838364
183	11.10068892	42.07688558	1765.251	2.30659E-15	22.8525718
184	11.22906035	42.04569514	1086.478	1.41966E-15	23.37953563
197	11.06755224	41.95098723	9058.132	1.1836E-14	21.07699136
199	11.09722105	41.89337201	6134.699	8.01601E-15	21.50010482
200	11.04995826	41.90324725	2273.122	2.97021E-15	22.57803111
201	10.99970817	41.84921165	7621.785	9.95913E-15	21.26444623
202	10.91122703	41.82541483	1582.959	2.0684E-15	22.9709138
203	10.90242311	41.8286875	8675.29	1.13357E-14	21.12387797
204	11.33991408	41.74361035	5360.234	7.00404E-15	21.6038323
205	11.08050669	41.7693089	4850.944	6.33857E-15	21.7587024
206	10.97862086	41.76101173	2267.753	2.9632E-15	22.5028299
207	11.02601564	41.76648743	2687.569	3.51176E-15	22.3230949
208	11.02113819	41.75416017	1062.297	1.38807E-15	23.2804578
209	10.97878959	41.73118005	2402.224	3.13891E-15	22.5107275
210	11.001357	41.73259943	8447.091	1.10375E-14	21.1627712
211	11.00891041	41.73787824	1515.82	1.98067E-15	22.9692496
212	11.0359336	41.72887911	1836.953	2.40029E-15	22.7402304
213	11.05191296	41.73887849	4029.802	5.26561E-15	21.9252646
214	11.03962799	41.71002864	950.9644	1.24259E-15	23.5545486
215	11.06780701	41.70636122	272.8912	3.56578E-16	24.870261
216	11.11516092	41.74151219	2692.367	3.51803E-15	22.3819648
217	11.15934766	41.73175062	2277.197	2.97554E-15	22.6048872
218	11.18557048	41.73696771	1655.809	2.16359E-15	23.0380083
219	11.22406659	41.70649196	6675.23	8.7223E-15	21.3984349
220	11.08388513	41.70084169	1147.296	1.49913E-15	23.228407
221	11.29271903	41.70733455	4352.646	5.68746E-15	21.872853
222	11.3516395	41.72647436	3576.766	4.67364E-15	22.066442
223	11.4833042	41.72134123	10462.63	1.36712E-14	20.9204858
224	11.42304688	41.71855713	2359.563	3.08316E-15	22.4704165
225	11.5721575	41.72471085	1630.165	2.13008E-15	22.93900906
226	11.50226293	41.65733073	1525.964	1.99393E-15	23.01072725
227	11.47431602	41.66555914	838.1332	1.09516E-15	23.66130536
228	11.36263515	41.68841048	3242.39	4.23672E-15	22.1577443
229	11.36125426	41.68022895	1019.977	1.33277E-15	23.337961
230	11.56600846	41.70058689	962.3488	1.25747E-15	23.5112567
231	11.52076828	41.66019875	541.4221	7.07458E-16	24.13574802
232	11.3268886	41.70450076	485.1263	6.33898E-16	24.1918051
234	11.05057097	41.66365993	1633.921	2.13499E-15	22.7371206
235	11.03935478	41.66659921	8576.978	1.12073E-14	21.1575561
236	11.08957594	41.66833288	1850.631	2.41816E-15	22.8409197
237	11.08851294	41.65825826	15114.72	1.97499E-14	20.5151169
239	11.25161493	41.65423679	11915.53	1.55696E-14	20.7872113
240	11.30150966	41.65579796	13904.06	1.8168E-14	20.6050819
241	11.0364173	41.65940682	4213.262	5.50533E-15	22.7709811
243	10.98539097	41.63601	2962.204	3.87061E-15	22.2896231
244	10.95683272	41.6355121	3666.93	4.79146E-15	22.0774754

Table B.1 (cont'd)

ID	RA (deg)	Dec (deg)	Flux (counts)	Flux (ergs/sec/cm ² /Å)	Mag
245	11.01611162	41.61462485	6566.508	8.58024E-15	21.4431696
246	11.10389134	41.64188682	5512.239	7.20266E-15	21.6228389
247	11.12738463	41.62917185	1254.225	1.63885E-15	23.1451176
248	11.01442238	41.6420643	5748.224	7.51101E-15	21.4846707
249	11.15416759	41.62399798	2423.227	3.16635E-15	22.4845215
250	11.24517928	41.61443641	2529.317	3.30497E-15	22.5096115
251	11.31001304	41.65096408	4761.348	6.22149E-15	21.7552549
252	11.45477092	41.6123729	2063.499	2.69631E-15	22.68307731
253	11.44522233	41.61618817	526.5966	6.88086E-16	24.16589284
254	11.59994249	41.64554307	1268.242	1.65717E-15	23.21158264
255	11.59769208	41.6369516	1192.827	1.55863E-15	23.27814432
256	11.46270235	41.58838751	7507.315	9.80956E-15	21.28087637
258	11.35903354	41.57968641	7738.452	1.01116E-14	21.2433646
259	11.34836014	41.59750107	5313.076	6.94242E-15	21.6490851
260	11.37043291	41.60415163	3368.943	4.40209E-15	22.1369897
261	11.35835058	41.60889249	1093.127	1.42835E-15	23.2787616
262	11.26347648	41.59789338	13765.82	1.79873E-14	20.6165687
263	11.22519117	41.58584786	2456.192	3.20942E-15	22.4658909
264	11.25054866	41.61212143	4750.835	6.20776E-15	21.7894845
265	11.09315627	41.59772308	8402.615	1.09794E-14	21.1235808
266	10.91700281	41.58470734	6065.949	7.92617E-15	21.5710812
267	10.91719562	41.60051671	1270.606	1.66026E-15	23.1908422
268	10.90196617	41.59716871	1699.334	2.22046E-15	22.8739465
269	10.95553478	41.59211535	1109.999	1.4504E-15	23.127697
270	10.97795686	41.58409543	1807.211	2.36142E-15	22.7392202
271	10.96378092	41.60601628	1920.716	2.50974E-15	22.6909722
272	10.9381791	41.58841505	1257.461	1.64308E-15	23.0772311
273	10.90211942	41.55078533	2200.158	2.87487E-15	22.7450527
274	11.01923013	41.5758039	9092.917	1.18814E-14	21.0106967
275	11.04685847	41.57351814	6449.982	8.42798E-15	21.4673973
276	11.07342032	41.56189513	5763.887	7.53148E-15	21.6183026
277	11.10952226	41.55422378	14628.38	1.91144E-14	20.5878502
278	11.1241586	41.54594416	5370.091	7.01692E-15	21.6659084
279	11.07787012	41.59225332	8419.146	1.1001E-14	21.1723996
280	11.14379681	41.55821182	10238.69	1.33786E-14	20.9635677
281	11.28935703	41.57516084	7989.937	1.04402E-14	21.1831151
282	11.33791408	41.55800748	5988.129	7.82449E-15	21.5217846
284	11.31699187	41.55152704	939.6444	1.2278E-15	23.7420268
285	11.44713099	41.58698612	727.9221	9.51152E-16	23.81437571
286	11.36698181	41.57635642	1089.282	1.42333E-15	23.341356
287	11.57619418	41.51950799	15344.16	2.00497E-14	20.50473017
288	11.50824119	41.52800399	1627.38	2.12644E-15	22.94086553
289	11.50386946	41.5222169	1124.046	1.46875E-15	23.34262776
290	11.36224157	41.53600132	2067.328	2.70131E-15	22.6420975
291	11.20903871	41.51893792	12966.88	1.69434E-14	20.7104463
292	11.20971869	41.53085496	3909.862	5.10889E-15	21.9680195
293	11.16180973	41.52545188	1848.332	2.41515E-15	22.7858828
294	11.17375656	41.53453467	3059.339	3.99754E-15	22.2494885

Table B.1 (cont'd)

ID	RA (deg)	Dec (deg)	Flux (counts)	Flux (ergs/sec/cm ² /Å)	Mag
295	11.18853247	41.53051554	3772.098	4.92887E-15	22.0324362
296	11.10405166	41.529471	7750.91	1.01279E-14	21.2460507
297	11.02677823	41.5343119	8983.065	1.17379E-14	21.1174386
298	11.03978415	41.53753093	3558.62	4.64993E-15	22.1196058
299	11.05604368	41.53172043	2292.81	2.99594E-15	22.662225
300	11.04569274	41.52969044	2947.222	3.85104E-15	22.2928961
301	11.06286902	41.54134271	2569.003	3.35683E-15	22.5104359
302	11.03402122	41.5220509	2889.104	3.7751E-15	22.6059482
303	10.9147204	41.53606757	5494.717	7.17976E-15	21.6726629
304	10.93622675	41.52183633	2874.674	3.75624E-15	22.4243742
305	10.95066499	41.52405615	5346.218	6.98572E-15	21.7894088
308	10.88807111	41.87944947	4584.033	5.9898E-15	21.81646863
309	10.9977307	41.82835026	1124.344	1.46914E-15	23.34233995
319	11.4260574	41.74147605	3837.736	5.01464E-15	22.0201985
320	11.38962554	41.74838936	816.4998	1.06689E-15	23.5902081
330	10.89775502	41.78151034	1048.094	1.36951E-15	23.41858738
331	10.96431954	41.76908154	1009.561	1.31916E-15	23.4269949
332	10.95343356	41.77726117	688.585	8.99751E-16	23.87469407
333	11.00553507	41.78578576	1288.218	1.68327E-15	23.19461456
337	11.05581004	41.72028117	880.3247	1.15029E-15	23.7214493
338	11.13233757	41.73684724	367.935	4.80768E-16	24.7372395
339	11.22272701	41.71802612	746.7077	9.75698E-16	23.6691035
341	11.18400544	41.73475724	2053.938	2.68381E-15	22.68811964
342	11.31202118	41.72971847	1243.43	1.62475E-15	23.2542077
343	11.30728425	41.7214262	1005.434	1.31377E-15	23.6077898
344	11.25828918	41.67741961	852.9418	1.11451E-15	23.6370958
345	10.98620303	41.70044495	1372.757	1.79374E-15	23.0721213
350	11.05087933	41.64481741	666.8749	8.71383E-16	23.7473394
351	11.12289434	41.65013835	752.1368	9.82792E-16	23.6426738
352	11.17063728	41.61860475	1217.098	1.59034E-15	23.2992008
353	11.07098097	41.6459209	2128.38	2.78108E-15	22.7229156
365	11.28972691	41.56058574	1487.168	1.94323E-15	23.0824718
366	11.22470451	41.56829098	407.3471	5.32267E-16	24.4676861
498	10.96124663	41.54778456	1042.44	1.36212E-15	23.5071537
242	11.03123518	41.6637851	478.3595	6.25056E-16	24.27020196
304	10.93626873	41.52184169	2500.881	3.26782E-15	22.4743554
305	10.95069842	41.52404367	4618.917	6.03538E-15	21.80823757
354	10.84842548	41.60316519	3380.471	4.41715E-15	22.14714493
355	10.86503018	41.62592349	1318.045	1.72225E-15	23.16976237
356	10.88063056	41.62435864	766.1829	1.00115E-15	23.75875683
357	10.79646047	41.61029667	3241.295	4.23529E-15	22.2006399
358	10.80893857	41.5910545	6190.586	8.08903E-15	21.5325731
359	10.80360466	41.59144039	3132.915	4.09368E-15	22.2716965
361	10.83302961	41.59218881	449.8363	5.87786E-16	24.2104404
362	10.83686594	41.61640785	714.1609	9.3317E-16	23.8350978
367	10.90496054	41.51805781	7182.708	9.38541E-15	21.3257551
368	10.81821331	41.54998544	10341.09	1.35124E-14	20.9713424
369	10.85989183	41.5292721	4253.247	5.55758E-15	21.8949981

Table B.1 (cont'd)

ID	RA (deg)	Dec (deg)	Flux (counts)	Flux (ergs/sec/cm ² /Å)	Mag
370	10.74714784	41.50828402	9218.018	1.20449E-14	21.0655202
371	10.73490387	41.49492443	2495.702	3.26105E-15	22.537641
372	10.76256737	41.49059189	4027.183	5.26219E-15	21.9243116
373	10.78307733	41.47928996	8843.216	1.15551E-14	21.0807395
375	10.79628958	41.5070584	2848.297	3.72177E-15	22.390434
376	10.81111967	41.50934147	2963.599	3.87244E-15	22.3460581
377	10.82272107	41.48811653	3697.755	4.83173E-15	22.0238921
378	10.83539851	41.48595046	2532.529	3.30917E-15	22.4487827
379	10.85901629	41.49379252	5215.091	6.81439E-15	21.6789003
380	10.84924938	41.50378364	2201.474	2.87659E-15	22.7594602
381	10.85085953	41.49805946	1301.785	1.701E-15	23.0313611
382	10.73311792	41.50211106	1121.918	1.46597E-15	23.4025589
383	10.75333346	41.5032868	6317.167	8.25443E-15	21.570488
385	10.86819197	41.49936922	1583.81	2.06951E-15	23.0429651
386	10.91513432	41.48848093	6829.203	8.92349E-15	21.3915496
387	10.93126451	41.51596332	6016.451	7.8615E-15	21.52123701
388	11.10207243	41.49640448	11710.82	1.53021E-14	20.8376363
389	11.05512007	41.50283312	3375.217	4.41028E-15	22.161522
390	11.10629554	41.49818784	2870.8	3.75118E-15	22.5409391
391	11.14429657	41.48811677	10151.27	1.32643E-14	20.987893
393	11.25599769	41.50528007	2305.431	3.01243E-15	22.56270765
394	11.15602908	41.45282971	9758.196	1.27507E-14	21.015757
395	11.10672966	41.44467193	16957.2	2.21574E-14	20.4286537
396	11.09709365	41.49260854	3070.321	4.01189E-15	22.2135292
397	11.06507293	41.45447579	4529.763	5.91889E-15	21.8272381
398	11.04029739	41.45352179	5733.557	7.49185E-15	21.5590516
399	11.01082345	41.46778087	5788.855	7.5641E-15	21.6105807
400	11.02842337	41.46842221	3024.646	3.9522E-15	22.3447583
401	10.99484324	41.45543616	3024.649	3.95221E-15	22.2552834
402	11.07132322	41.49690123	3133.959	4.09504E-15	22.2422298
403	10.86216568	41.47247649	9653.982	1.26145E-14	21.0254355
404	10.81911101	41.44091029	4006.511	5.23517E-15	22.0436298
405	10.81698511	41.45113345	7025.089	9.17945E-15	21.3934041
406	10.95659252	41.46602903	3657.065	4.77856E-15	22.1467831
407	10.92332187	41.46727521	3420.088	4.46891E-15	22.2081538
408	10.92505296	41.47753926	1048.45	1.36997E-15	23.4935493
409	10.91313745	41.44155429	3337.347	4.3608E-15	22.1319669
410	10.97105247	41.46591764	1757.823	2.29689E-15	22.7482964
411	10.74455282	41.46322828	9172.61	1.19855E-14	21.0868709
412	10.7489223	41.46905239	1114.824	1.4567E-15	23.3590999
413	10.79020291	41.44760648	2484.281	3.24613E-15	22.4837027
414	10.79105866	41.45205672	4166.986	5.44486E-15	21.8967046
415	10.68729648	41.46553578	4230.036	5.52725E-15	21.8710454
416	10.65673357	41.4299133	1746.473	2.28206E-15	23.0069624
417	10.70494601	41.43204112	5689.983	7.43491E-15	21.5875436
418	10.7396262	41.40928548	5373.841	7.02182E-15	21.6254051
419	10.79465074	41.42782669	10405.4	1.35964E-14	20.9844729
420	10.77905483	41.41550957	3677.463	4.80522E-15	22.1104333

Table B.1 (cont'd)

ID	RA (deg)	Dec (deg)	Flux (counts)	Flux (ergs/sec/cm ² /Å)	Mag
421	10.80479787	41.40625993	5860.955	7.65831E-15	21.6001022
422	10.74284947	41.41964283	3476.25	4.5423E-15	22.0963459
423	10.90821214	41.40937967	6047.045	7.90147E-15	21.5623131
424	11.03066922	41.42572528	7085.396	9.25825E-15	21.3380297
425	11.13406323	41.42986261	6067.377	7.92804E-15	21.50553986
426	11.09951259	41.43846999	5778.278	7.55028E-15	21.6003402
427	11.05585452	41.41843816	2658.571	3.47387E-15	22.386516
428	11.09862922	41.43115352	1756.49	2.29515E-15	22.7879784
429	11.16509549	41.42819514	8293.285	1.08366E-14	21.2887392
430	11.26227791	41.42444631	11476.77	1.49963E-14	20.82003877
431	11.23771204	41.4381227	2617.146	3.41974E-15	22.42501809
438	11.04325905	41.40507175	9610.754	1.25581E-14	21.0199201
439	11.08683752	41.40759446	4994.747	6.52647E-15	21.7554668
440	10.9092602	41.40155248	3707.598	4.84459E-15	22.1264942
441	10.8509675	41.41044457	5054.5	6.60455E-15	21.8127412
442	10.85215231	41.39567783	3439.692	4.49453E-15	22.1403369
443	10.84740802	41.39769104	2398.382	3.13389E-15	22.4829354
444	10.69098897	41.39284741	4286.919	5.60157E-15	21.8604265
445	10.89745834	41.37506155	5327.771	6.96162E-15	21.6505889
446	10.91404952	41.38273988	5071.604	6.6269E-15	21.7217196
447	10.95716612	41.37845386	7390.556	9.65699E-15	21.3361206
448	10.97650019	41.39249969	8411.986	1.09917E-14	21.199115
449	11.00909335	41.38089572	2370.173	3.09703E-15	22.5292326
450	11.02168746	41.38618907	2850.8	3.72505E-15	22.3196761
451	11.11461768	41.37478996	2453.799	3.2063E-15	22.4393921
452	11.11789933	41.38832547	4244.94	5.54672E-15	21.9311041
453	11.1127159	41.40036764	678.718	8.86858E-16	23.5067326
454	11.05673435	41.39234535	2162.243	2.82533E-15	22.5906427
456	11.06611171	41.36974479	5410.864	7.0702E-15	21.611889
457	11.13077076	41.35884425	9074.191	1.18569E-14	21.1275884
458	10.97823221	41.36814093	3593.156	4.69506E-15	22.1457564
459	10.98426019	41.37062153	11660.19	1.5236E-14	20.8208552
460	10.99695663	41.36355955	2392.537	3.12625E-15	22.5490129
461	10.85224228	41.36789431	4761.744	6.22201E-15	21.7878575
462	10.8022605	41.35485855	9887.419	1.29196E-14	20.9942107
463	10.84672905	41.36588487	9552.121	1.24814E-14	21.0038276
464	10.82502337	41.35973539	6073.395	7.9359E-15	21.5452895
465	10.72707438	41.35659926	10459.71	1.36674E-14	20.906874
466	10.86092924	41.34083482	8166.728	1.06712E-14	21.1884569
467	10.86846888	41.33842682	7762.135	1.01425E-14	21.2808372
468	10.92997655	41.33949196	6511.731	8.50866E-15	21.4833204
469	10.9940223	41.32325687	6369.751	8.32314E-15	21.4514198
470	11.00695889	41.32763147	3789.929	4.95217E-15	22.0471027
471	11.05109478	41.34464458	1277.108	1.66875E-15	23.1053895
472	11.07013222	41.36210288	2801.589	3.66074E-15	22.2593428
476	11.06745649	41.31480676	12683.6	1.65732E-14	20.7117963
477	11.02359132	41.30086123	4970.974	6.49541E-15	21.7594274
478	10.93159826	41.3204982	5735.253	7.49406E-15	21.5993154

Table B.1 (cont'd)

ID	RA (deg)	Dec (deg)	Flux (counts)	Flux (ergs/sec/cm ² /Å)	Mag
479	10.96787906	41.31424618	2599.159	3.39623E-15	22.4364152
480	10.92208411	41.30335366	3649.205	4.76829E-15	22.0711035
481	10.88637608	41.30918182	6593.219	8.61514E-15	21.3928884
482	10.8370228	41.29785285	6671.696	8.71768E-15	21.4167306
483	10.99757423	41.27990903	4693.55	6.13291E-15	21.740034
484	11.13458025	41.29610066	1385.141	1.80992E-15	23.0367839
486	10.77630069	41.58694588	572.9917	7.48709E-16	23.8920831
487	10.72131166	41.60602049	1392.454	1.81947E-15	23.11013583
496	10.80105912	41.55453749	1647.981	2.15336E-15	22.8789947
497	10.81494492	41.56331734	965.5662	1.26167E-15	23.3363685
500	10.65817863	41.47128493	493.3036	6.44583E-16	24.0681764
501	10.66897011	41.45891521	854.1413	1.11608E-15	23.5234057
511	10.73672209	41.45739577	2116.805	2.76596E-15	22.6484349
512	10.67147412	41.40626321	941.1976	1.22983E-15	23.5578635
513	10.73917105	41.38488136	4374.408	5.71589E-15	21.9080526
519	10.74516558	41.37046335	5230.586	6.83463E-15	21.6837818
520	10.73404594	41.36760091	5186.063	6.77646E-15	21.6334623
521	10.90520802	41.37727005	3142.306	4.10595E-15	22.2930958
522	11.04485455	41.30398241	3623.438	4.73463E-15	22.1289991
523	10.89306216	41.32648294	3611.364	4.71885E-15	22.1942536
524	10.78049812	41.32292552	9697.025	1.26708E-14	21.0283024
525	10.77762915	41.31060097	7070.708	9.23906E-15	21.3754142
526	10.74298958	41.28622786	15775.25	2.0613E-14	20.4915103
527	10.78671005	41.33369237	5657.723	7.39276E-15	21.6458268
364	10.72340427	41.57929224	2432.735	3.17877E-15	22.50435096
475	11.19564636	41.30027147	1028.754	1.34424E-15	23.43880913
493	10.62820829	41.5878391	1330.876	1.73901E-15	23.15924399
499	10.60933709	41.51701228	2308.582	3.01655E-15	22.56122471
502	10.63840166	41.50976146	2784.933	3.63898E-15	22.35755109
506	10.46807559	41.42568435	2488.707	3.25191E-15	22.47965355
507	10.55233126	41.43819224	1758.652	2.29797E-15	22.85663819
508	10.58981607	41.42216371	2764.44	3.6122E-15	22.36557005
509	10.57018285	41.41028781	1312.5	1.715E-15	23.17433969
510	10.59026933	41.46237615	1077.488	1.40792E-15	23.38855686
514	10.50615165	41.40590026	6811.114	8.89986E-15	21.3865426
515	10.59576851	41.38516556	8319.539	1.08709E-14	21.16933981
517	10.57322201	41.34229903	1880.364	2.45701E-15	22.78398315
518	10.54315201	41.34594211	774.4457	1.01194E-15	23.74711054
528	10.60069234	41.33631241	3610.302	4.71746E-15	22.07572914
529	10.53458035	41.32486337	1474.373	1.92651E-15	23.04806955
532	10.46812123	41.26192838	5979.152	7.81276E-15	21.52798898
533	10.52183565	41.26941642	7529.608	9.83869E-15	21.27765705
534	10.54815788	41.26987945	1296.935	1.69466E-15	23.18729244
535	10.57768042	41.24906183	4047.922	5.28928E-15	21.95150763
536	10.59318521	41.26788892	10964.9	1.43275E-14	20.86957628
537	10.58663706	41.28158006	8405.104	1.09827E-14	21.15823024
538	10.61569198	41.27534596	14360.6	1.87645E-14	20.57665651
539	10.78957636	41.26474485	12213.34	1.59588E-14	20.75250185

Table B.1 (cont'd)

ID	RA (deg)	Dec (deg)	Flux (counts)	Flux (ergs/sec/cm ² /Å)	Mag
540	10.86898567	41.26265508	4918.802	6.42723E-15	21.73993962
541	10.82940844	41.25272586	7981.312	1.04289E-14	21.21440225
542	10.82012626	41.2540599	3090.365	4.03808E-15	22.24456353
543	10.90398895	41.25265798	3670.172	4.79569E-15	22.05787193
544	10.90543043	41.24173668	6938.494	9.0663E-15	21.36642493
545	10.84595514	41.26128538	2670.578	3.48956E-15	22.4030748
546	10.93121844	41.24818488	1777.254	2.32228E-15	22.84521422
547	10.99951912	41.25982848	3329.856	4.35101E-15	22.16352434
552	11.0496031	41.23337075	5085.703	6.64532E-15	21.70371048
553	11.01916229	41.202468	5297.266	6.92176E-15	21.65945852
554	11.0390049	41.21837059	1217.874	1.59136E-15	23.25558207
555	11.0582682	41.20830403	1982.07	2.5899E-15	22.7267905
556	11.03840172	41.19629825	1130.422	1.47708E-15	23.33648647
557	11.04485653	41.20988362	1450.027	1.8947E-15	23.06614775
559	10.82992938	41.20365884	4086.542	5.33975E-15	21.94119805
560	10.80161005	41.21215847	6837.178	8.93391E-15	21.38239575
561	10.74496455	41.21401129	7174.516	9.3747E-15	21.33010645
562	10.74102222	41.21206566	6924.63	9.04818E-15	21.36859654
563	10.71592259	41.20412717	12334.37	1.61169E-14	20.74179554
564	10.55775358	41.22681054	14751.05	1.92747E-14	20.54753063
565	10.6132466	41.24289561	11165.44	1.45895E-14	20.84989836
566	10.59096957	41.23643893	9053.343	1.18297E-14	21.07756553
567	10.6944237	41.22125249	10565.35	1.38054E-14	20.90987825
568	10.71964333	41.23771357	11068.6	1.4463E-14	20.85935624
569	10.65393651	41.20264598	7627.128	9.96611E-15	21.26368538
570	10.55248245	41.22371575	4698.479	6.13935E-15	21.78969474
571	10.57923957	41.23427308	41930.65	5.47894E-14	19.41325898
572	10.59663928	41.2270487	2789.385	3.6448E-15	22.35581682
573	10.60184314	41.20320418	5806.567	7.58725E-15	21.55978937
574	10.6081569	41.20872307	6695.977	8.74941E-15	21.40505309
575	10.54294002	41.21046573	11565.68	1.51125E-14	20.81166004
576	10.53204452	41.22457551	4481.412	5.85571E-15	21.84105079
577	10.52582979	41.23999164	5899.002	7.70803E-15	21.54264161
578	10.47729394	41.22369479	2293.84	2.99728E-15	22.56818016
579	10.47349951	41.22336918	1929.995	2.52186E-15	22.75569751
580	10.4943753	41.20123062	3389.787	4.42932E-15	22.14415694
581	10.50994026	41.24087686	1627.55	2.12667E-15	22.94075212
582	10.44094134	41.17693775	1505.334	1.96697E-15	23.02550579
583	10.44578747	41.17201504	1774.475	2.31865E-15	22.84691326
584	10.45740037	41.16366707	2012.414	2.62955E-15	22.71029464
585	10.4569857	41.18939708	3240.566	4.23434E-15	22.19303579
586	10.52760379	41.19257689	4284.222	5.59805E-15	21.88990805
587	10.49034253	41.16211785	4330.855	5.65898E-15	21.87815386
588	10.63589389	41.17085845	9026.385	1.17945E-14	21.08080334
589	10.61816617	41.16580173	6452.192	8.43086E-15	21.44531976
590	10.61266095	41.16256835	5464.891	7.14079E-15	21.62563421
591	10.62293594	41.18060461	6665.641	8.70977E-15	21.40998317
592	10.59218952	41.19058622	4012.76	5.24334E-15	21.96098

Table B.1 (cont'd)

ID	RA (deg)	Dec (deg)	Flux (counts)	Flux (ergs/sec/cm ² /Å)	Mag
593	10.68282745	41.17973235	12933.97	1.69004E-14	20.69025835
594	10.64915129	41.18374988	4110.288	5.37078E-15	21.93490734
595	10.73502677	41.2247321	23275.29	3.0413E-14	20.05235022
596	10.77578634	41.1821986	9513.167	1.24305E-14	21.02377517
597	10.84578894	41.18082849	4437.025	5.79771E-15	21.85185828
598	10.76371594	41.20325161	1764.111	2.30511E-15	22.8532732
599	10.78259553	41.2088085	2173.699	2.8403E-15	22.62658946
600	10.97948654	41.18588391	1506.981	1.96912E-15	23.02431853
601	10.99505735	41.19178012	2492.337	3.25665E-15	22.47807106
605	11.02043422	41.15521078	3862.061	5.04643E-15	22.00254015
607	10.91547389	41.14883703	5156.123	6.73733E-15	21.6887798
608	10.94234214	41.14820092	4827.909	6.30847E-15	21.76019028
609	10.95435516	41.16085771	1868.953	2.4421E-15	22.79059202
610	10.96811875	41.15175497	1689.716	2.2079E-15	22.90005368
611	10.85380207	41.16579351	3236.572	4.22912E-15	22.19437479
612	10.86265463	41.17458865	7437.165	9.7179E-15	21.29106943
613	10.76071401	41.14537411	4282.346	5.5956E-15	21.89038358
614	10.71455009	41.14924888	2685.996	3.5097E-15	22.39682457
615	10.72259127	41.14951354	1726.743	2.25628E-15	22.87651871
616	10.67882192	41.15648643	7119.522	9.30284E-15	21.33846088
617	10.67862691	41.16321339	3101.656	4.05283E-15	22.2406039
618	10.67306512	41.16651143	3593.568	4.6956E-15	22.0807733
619	10.65990504	41.16650816	3253.756	4.25157E-15	22.18862551
620	10.65903281	41.16554509	1932.249	2.52481E-15	22.75443024
621	10.59056972	41.16537156	5062.398	6.61487E-15	21.70869725
622	10.58837139	41.1621167	2886.015	3.77106E-15	22.31884151
623	10.61877018	41.15978353	5930.367	7.74901E-15	21.53688404
624	10.54091607	41.19854914	2174.827	2.84177E-15	22.62602618
625	10.56913123	41.18538564	3511.762	4.5887E-15	22.10577528
626	10.50057631	41.15478457	3062.932	4.00223E-15	22.25424458
627	10.49210077	41.13623411	6658.047	8.69985E-15	21.41122083
628	10.45889469	41.12617069	3255.962	4.25446E-15	22.18788965
629	10.42084385	41.1154943	3716.175	4.8558E-15	22.04434758
630	10.46550453	41.12795732	396.9516	5.18683E-16	24.47274408
631	10.50673799	41.12221112	4150.53	5.42336E-15	21.92432908
632	10.53532128	41.12666274	2867.21	3.74649E-15	22.32593921
633	10.54244382	41.12200101	3144.628	4.10898E-15	22.22566478
634	10.54526981	41.12091807	332.8384	4.34909E-16	24.66400441
635	10.55102593	41.12420122	6170.137	8.06231E-15	21.49385095
636	10.60131912	41.11984837	6262.079	8.18245E-15	21.47779161
637	10.60262686	41.12455441	5358.609	7.00192E-15	21.6469578
638	10.58514842	41.13326034	9704.377	1.26804E-14	21.00216882
639	10.61174999	41.121745	1923.121	2.51288E-15	22.75957144
640	10.62054437	41.12026243	5002.946	6.53718E-15	21.72152343
641	10.63062293	41.12979372	2849.949	3.72393E-15	22.33249525
642	10.59950096	41.14196102	2969.591	3.88027E-15	22.28784637
643	10.70610489	41.14004634	3454.19	4.51347E-15	22.12372241
644	10.76515969	41.09270304	3773.749	4.93103E-15	22.02765544

Table B.1 (cont'd)

ID	RA (deg)	Dec (deg)	Flux (counts)	Flux (ergs/sec/cm ² /Å)	Mag
645	10.83881885	41.09144934	16967.91	2.21714E-14	20.39551709
646	10.84354499	41.12203013	6378.904	8.3351E-15	21.4577228
647	10.85246007	41.12120722	1613.875	2.1088E-15	22.94991323
648	10.8600225	41.1118831	3042.909	3.97607E-15	22.26136556
649	10.77691483	41.12305378	3268.033	4.27023E-15	22.18387189
650	10.74972874	41.09587218	1736.573	2.26912E-15	22.87035536
651	10.7826246	41.08700476	3126.005	4.08465E-15	22.2321138
652	10.61970827	41.10589054	7173.353	9.37318E-15	21.33028246
653	10.62676105	41.09780791	3902.744	5.09959E-15	21.99116281
654	10.64111824	41.09476077	1611.708	2.10597E-15	22.95137207
655	10.6011218	41.096852	4633.941	6.05502E-15	21.80471172
656	10.59182185	41.09889244	2291.512	2.99424E-15	22.56928263
657	10.45030771	41.09894279	3386.48	4.425E-15	22.14521668
658	10.48651828	41.10357091	2775.142	3.62619E-15	22.36137494
659	10.50107902	41.1009424	3193.103	4.17232E-15	22.20905565
660	10.45413191	41.07390019	1447.962	1.892E-15	23.06769506
661	10.52939808	41.0625846	3733.916	4.87898E-15	22.03917661
662	10.43290883	41.07680312	5619.518	7.34284E-15	21.5953403
663	10.52837543	41.07152557	7507.902	9.81033E-15	21.28079148
664	10.62397876	41.05849369	8564.623	1.11911E-14	21.13781734
665	10.56541827	41.06079547	2993.513	3.91152E-15	22.2791351
666	10.65506906	41.07212094	3509.523	4.58578E-15	22.10646774
667	10.78938379	41.08147608	4527.73	5.91623E-15	21.82988667
668	10.81326427	41.07272633	11911.65	1.55646E-14	20.77965816
669	10.83263817	41.04288405	4452.813	5.81834E-15	21.84800183
670	10.73177519	41.0614638	2956.732	3.86346E-15	22.29255807
671	10.74248981	41.06512699	868.3568	1.13465E-15	23.62284245
675	10.70847948	41.03915802	111.8311	1.46126E-16	25.84818148
676	10.434891	41.03650825	5665.431	7.40283E-15	21.58650558
677	10.44172703	41.0380653	2979.768	3.89356E-15	22.28413184
678	10.44190905	41.05342938	8018.91	1.0478E-14	21.20929962
679	10.50228034	41.03512056	3199.542	4.18073E-15	22.20686843
680	10.47403186	41.02557714	2943.043	3.84558E-15	22.29759645
681	10.50735679	41.05735359	1881.102	2.45797E-15	22.78355711
682	10.51583103	41.0551633	1898.01	2.48007E-15	22.77384173
683	10.46524246	41.08029021	1161.714	1.51797E-15	23.30683991
684	10.58029188	41.08113562	1804.276	2.35759E-15	22.82883054
685	10.50773316	41.13187712	2536.256	3.31404E-15	22.45910525

APPENDIX C

LETTER FROM INSTITUTIONAL RESEARCH BOARD



Office of Research Integrity

December 2, 2016

Dr. Maria Babiuc Hamilton
Department of Physics
251 Science Building
Marshall University

Dear Dr. Hamilton:

This letter is in response to the submitted thesis abstract for Yasaman Kahvaz entitled "*Planetary Nebula Associations With Star Clusters in the Andromeda Galaxy.*" After assessing the abstract it has been deemed not to be human subject research and therefore exempt from oversight of the Marshall University Institutional Review Board (IRB). The Code of Federal Regulations (45CFR46) has set forth the criteria utilized in making this determination. Since the information in this study does not involve human subjects as defined in the above referenced instruction it is not considered human subject research. If there are any changes to the abstract you provided then you would need to resubmit that information to the Office of Research Integrity for review and a determination.

I appreciate your willingness to submit the abstract for determination. Please feel free to contact the Office of Research Integrity if you have any questions regarding future protocols that may require IRB review.

Sincerely,

Bruce F. Day, ThD, CIP
Director

WE ARE... MARSHALL.

One John Marshall Drive • Huntington, West Virginia 25755 • Tel 304/696-4303
A State University of West Virginia • An Affirmative Action/Equal Opportunity Employer

REFERENCES

- [1] Ahad O Allakhverdiyev, Mehmet Ali Alpar, Oktay H Guseinov, and Enis Tuncer, *Planetary nebulae in open clusters and the mass boundary between the progenitors of white dwarfs and neutron stars*, *Astronomical and Astrophysical Transactions* **16** (1998), no. 1, 41–47.
- [2] C Moni Bidin, Daniel Majaess, Charles Bonatto, Francesco Mauro, David Turner, Doug Geisler, A-N Chené, Alex C Gormaz-Matamala, Jura Borissova, Radostin Georgiev Kurtev, et al., *Investigating potential planetary nebula/cluster pairs*, *Astronomy & Astrophysics* **561** (2014), A119.
- [3] Robin Ciardullo, George H Jacoby, Holland C Ford, and James D Neill, *Planetary nebulae as standard candles. ii-the calibration in m31 and its companions*, *The Astrophysical Journal* **339** (1989), 53–69.
- [4] Julianne J Dalcanton, Benjamin F Williams, Dustin Lang, Tod R Lauer, Jason S Kalirai, Anil C Seth, Andrew Dolphin, Philip Rosenfield, Daniel R Weisz, Eric F Bell, et al., *The panchromatic hubble andromeda treasury*, *The Astrophysical Journal Supplement Series* **200** (2012), no. 2, 18.
- [5] Morgan Fouesneau, L Clifton Johnson, Daniel R Weisz, Julianne J Dalcanton, Eric F Bell, Luciana Bianchi, Nelson Caldwell, Dimitrios A Gouliermis, Puragra Guhathakurta, Jason Kalirai, et al., *The panchromatic hubble andromeda treasury. v. ages and masses of the year 1 stellar clusters*, *The Astrophysical Journal* **786** (2014), no. 2, 117.
- [6] Martin Griffiths, *Planetary nebulae and how to observe them*, 1 ed., ‘Astronomers’ Observing Guides, vol. XV,287, Springer-Verlag New York, 2012.
- [7] George H Jacoby, Robin Ciardullo, Orsola De Marco, Myung Gyoon Lee, Kimberly A Herrmann, Ho Seong Hwang, Evan Kaplan, and James E Davies, *A survey for planetary nebulae in m31 globular clusters*, *The Astrophysical Journal* **769** (2013), no. 1, 10.
- [8] Daniel J Majaess, David G Turner, and David J Lane, *In search of possible associations between planetary nebulae and open clusters*, *Publications of the Astronomical Society of the Pacific* **119** (2007), no. 862, 1349–1360.
- [9] Philip Massey, Reagin T McNeill, KAG Olsen, Paul W Hodge, Cynthia Blaha, George H Jacoby, RC Smith, and Shay B Strong, *A survey of local group galaxies currently forming stars. iii. a search for luminous blue variables and other h α emission-line stars*, *The Astronomical Journal* **134** (2007), no. 6, 2474.
- [10] Quentin A Parker, Agnès Acker, David J Frew, Malcolm Hartley, Alan EJ Peyaud, François Ochsenbein, Steven Phillipps, Delphine Russeil, Sylvie F Beaulieu, M Cohen, et al., *The macquarie/aao/strasbourg h α planetary nebula catalogue: Mash*, *Monthly Notices of the Royal Astronomical Society* **373** (2006), no. 1, 79–94.
- [11] Barbara Ryden and Bradley M Peterson, *Foundations of astrophysics*, vol. 393-408, Addison-Wesley, 2010.

- [12] Mark J Veyette, Benjamin F Williams, Julianne J Dalcanton, Bruce Balick, Nelson Caldwell, Morgan Fouesneau, Léo Girardi, Karl D Gordon, Jason Kalirai, Philip Rosenfield, et al., *Panchromatic hubble andromeda treasury. ix. a photometric survey of planetary nebulae in m31*, The Astrophysical Journal **792** (2014), no. 2, 121.
- [13] Benjamin F Williams, Dustin Lang, Julianne J Dalcanton, Andrew E Dolphin, Daniel R Weisz, Eric F Bell, Luciana Bianchi, Nell Byler, Karoline M Gilbert, Léo Girardi, et al., *The panchromatic hubble andromeda treasury. x. ultraviolet to infrared photometry of 117 million equidistant stars*, The Astrophysical Journal Supplement Series **215** (2014), no. 1, 9.

Yasmine Kahvaz

Born September 12, 1988 in Iran.

Education

- Master of Physical and Applied Science. Marshall University, December 2016. Thesis Advisor: Timothy Hamilton.
- Bachelor of Science. Marshall University, May 2012.

Publications

1. *THE YOUNG SOLAR ANALOGS PROJECT. I. SPECTROSCOPIC AND PHOTOMETRIC METHODS AND MULTI-YEAR TIMESCALE SPECTROSCOPIC RESULTS.* R. O. Gray, J. M. Saken, C. J. Corbally, M. M. Briley, R. A. Lambert, V. A. Fuller, I. M. Newsome, M. F. Seeds, Y. Kahvaz. *The Astronomical Journal* (2015 December) 150:203 (19pp).
2. *Planetary Nebula Associations With Star Clusters in the Andromeda Galaxy.* Master's thesis, Marshall University, December 2016.